Chapter 3

Discovery of Orphan Receptor Tie1 and Angiopoietin Ligands Ang1 and Ang4 as Novel GAG-Binding Partners

3.1 Abstract

The Tie/Ang signaling axis is necessary for proper vascular development and remodeling. However, the mechanisms that modulate signaling through this receptor tyrosine kinase pathway are relatively unclear. In particular, the role of the orphan receptor Tie1 is highly disputed. Although this protein is required for survival, Tie1 has been found both to inhibit and yet be necessary for Tie2 signaling. While differing expression levels have been put forth as an explanation for its context-specific activity, the lack of known endogenous ligands for Tie1 has severely hampered understanding its molecular mode of action. Here we describe the discovery of orphan receptor Tie1 and angiopoietin ligands Ang1 and Ang4 as novel GAG binding partners. We localize the binding site of GAGs to the *N*-terminal region of Tie1, which may provide structural insights into the importance of this interaction regarding the formation of Tie1-Tie2 heterodimerization. Furthermore, we use our mutagenesis studies to guide the generation of a mouse model that specifically ablates GAG-Tie1 binding *in vivo* for further characterization of the functional outcomes of GAG-Tie1 binding. We also show that GAGs can form a trimeric complex with Ang1/4 and Tie2 using our microarray technology. Finally, we use our HaloTag glycan engineering platform to modify the cell surface of endothelial cells and demonstrate that HS GAGs can potentiate Tie2 signaling in a sulfation-specific manner, providing the first evidence of the involvement of HS GAGs in Tie/Ang signaling and delineating further the integral role of HS GAGs in angiogenesis.

3.1 Tie/Ang Signaling in Developing, Mature, and Remodeling Vasculature

Discovered in 1992, the Tie family of proteins is part of the RTK superfamily and consists of two members: Tie1 and Tie2 (Figure 3-1).[1-4] Along with the related angiopoietin (Ang or Angpt) ligands Ang1, Ang2, and Ang4,[5-7] the Tie/Ang signaling pathway is critical for the proper formation and maintenance of the vascular system.[8-10] Initial studies of Tie1 and Tie2 found that constitutive knockout of either receptor led to severe subcutaneous edema and tissue swelling, causing embryonic lethality for Tie2-deficient mice between embryonic days 10.5 and 12.5 (E10.5 - E12.5) and for Tie1-deficient mice starting at E13.5.[11-13] Tie1-deficient embryos that did not die *in utero* died upon birth due to respiratory failure likely caused by fluid accumulation in the lungs. Closer examination of the embryos showed stunted blood vessel networks, providing a possible mechanism for the edemic phenotype. Later studies linked the loss of Tie1 with impaired lymphogenesis via improper valve and collecting vessel development.[14-16] Moreover, Tie1 has been linked to numerous pathologies including tumor angiogenesis and atherosclerosis,[17, 18] and Tie/Ang proteins have been targeted as both anti-angiogenic and anti-sepsis therapeutics,[19, 20] illustrating the widespread importance of Tie/Ang signaling.

The Tie/Ang signaling axis shares some mechanistic similarities with other RTKs. For example, Tie2 is activated by dimerization or multimerization through binding to Ang1 or Ang4, leading to cross-phosphorylation of its intracellular domains and downstream signaling through the PI3K/Akt survival pathway.[9]

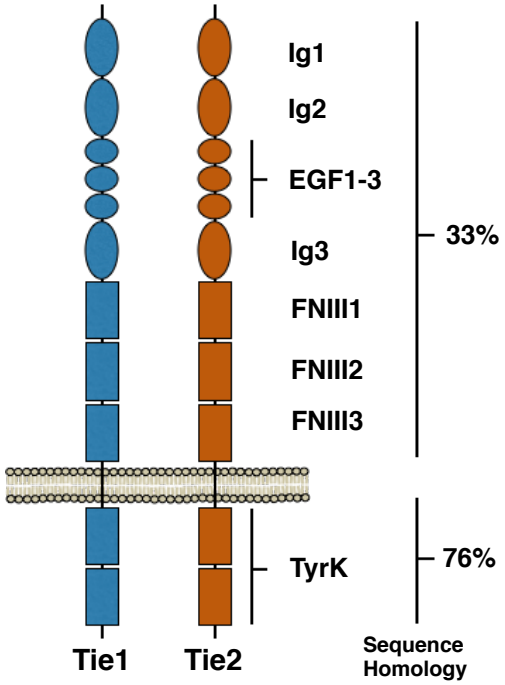

Figure 3-1. Domain structures of receptor tyrosine kinases Tie1 and Tie2.

However, Tie2 signaling is different from many other RTKs in that the protein is constantly activated in mature vessels. Ang1 is secreted by pericytes that surround vascular endothelial cells, activating Tie2 to promote cell survival (Figure 3-2). During angiogenesis, pericytes dissociate from the endothelial cells, which then produce Ang2 for autocrine antagonism of Tie2 survival signaling. If new blood vessels form with intact pericyte layers, pro-survival Tie2 signaling through Ang1 resumes. If unsuccessful, endothelial cells undergo apoptosis due to the lack of survival signaling.[9] The effect of Ang4, which appears to be human-specific and functionally distinct from its mouse ortholog Ang3,[7, 21] remains relatively unknown compared to Ang1 and Ang2.

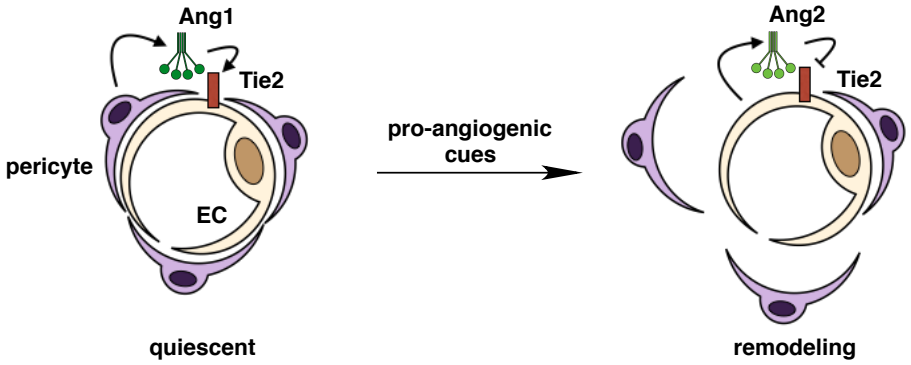

Figure 3-2. General mechanism of Tie/Ang signaling. In quiescent vasculature, Ang1 is secreted by pericytes to activate Tie2 on endothelial cells (EC). Upon receiving pro-angiogenic cues like VEGF, pericytes dissociate from ECs, which then secrete Ang2 to antagonize Ang1/Tie2 signaling.

Unlike Tie2, Tie1 is considered an orphan receptor.[9, 22, 23] Without a physiological ligand, its importance in vascular development and remodeling has proven much more difficult to unravel. Tie1 is generally though of as an antagonist of Tie2 signaling through the formation of Tie1/Tie2 heterodimers.[24] Experiments using shRNA-mediated knockdown of Tie1 demonstrated that Tie2 activation by Ang1 is elevated after depletion of Tie1.[25] However, a recent *in vivo* study showed that endothelial deletion of Tie1 in adult mice paradoxically leads to decreased Tie2 activation and downstream signaling,[26] suggesting instead that the Tie1/Tie2 interaction is necessary to promote Ang1-mediated vascular responses. In a separate report, Tie1 was suggested to both sustain and inhibit Tie2 function in different physical locations of newly forming blood vessels through changes in Tie1 expression levels.[22] However, a separate way to account for these differences in activity could be the presence of an undiscovered ligand for Tie1. GAGs are prevalent on the cell surface of most cells including the

endothelium and have previously been shown to bind both to RTKs and their respective ligands,[27-36] making them an ideal candidate for binding to not only Tie1 but also Ang ligands. Moreover, given the prevalence of GAG-RTK interactions in other systems involved in angiogenesis including VEGF/VEGFR,[29, 37] it is not difficult to envision the involvement of GAGs in the Tie/Ang signaling axis.

3.2 GAGs Are Physiological Ligands for Orphan Receptor Tie1

3.2.1 ELISA, Carbohydrate Microarray, and Surface Plasmon Resonance

We first examined whether Tie1 and Tie2 were receptors for GAGs using our carbohydrate enzyme-linked immunosorbent assay (ELISA) method.[38] Here, commercially available Tie1- and Tie2-Fc conjugates were immobilized onto Protein A/G coated plates. Biotinylated CS-E and trisulfated hep/HS (HS) were then incubated with the immobilized proteins for 3 h at RT, and bound GAGs were visualized using horseradish peroxidase (HRP)-conjugated streptavidin. Excitingly, we found that both CS-E and HS bound strongly to Tie1, both with nanomolar binding affinity (Figure 3-3; CS-E: 19.9 ± 5.8 nM, HS: 6.16 ± 0.37 nM). These data represent the first evidence of a physiological ligand for the Tie1 receptor since its discovery 25 years ago.[2] Furthermore, we found that Tie2 did not exhibit any measurable binding to either GAG structure, illustrating the specificity of the Tie1-GAG interaction.

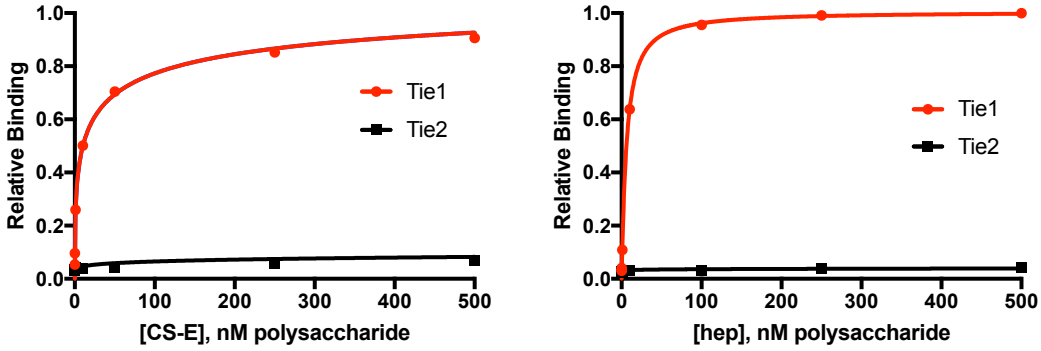

Figure 3-3. Carbohydrate enzyme-linked immunosorbent assay for Tie1-GAG binding. Immobilized Tie1-Fc or Tie2-Fc were probed with biotinylated CS-E or biotinylated HS.

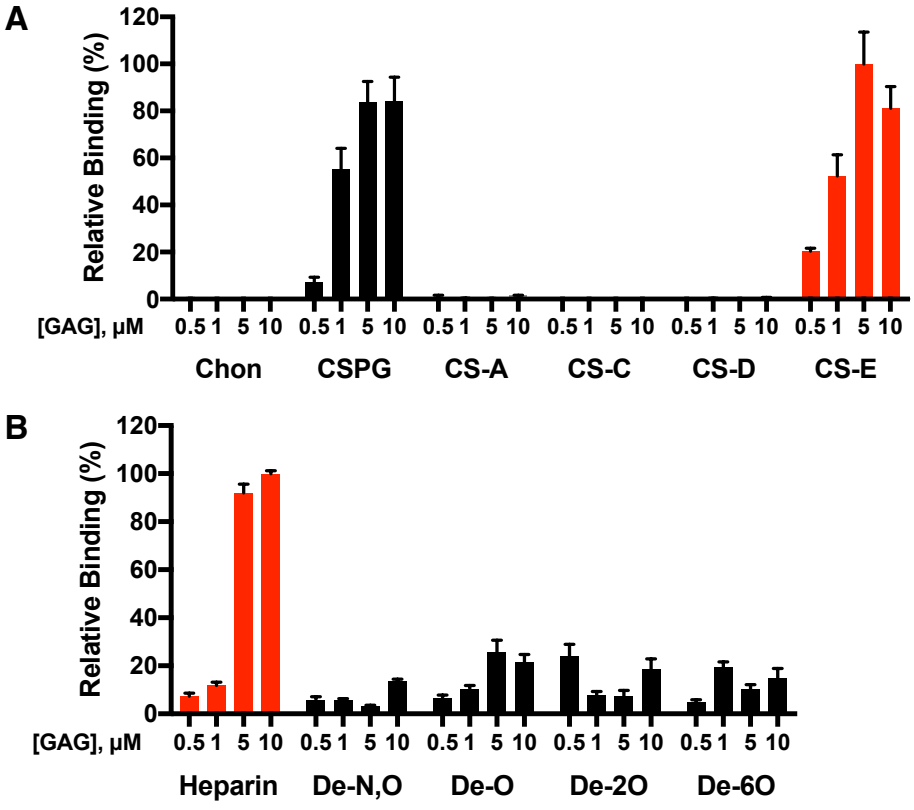

Figure 3-4. Carbohydrate microarrays to examine sulfation specificity of Tie1-GAG binding. Tie1-Fc was incubated with printed (A) CS and (B) HS microarray. Bound Tie1-Fc is visualized with an anti-human Fc antibody.

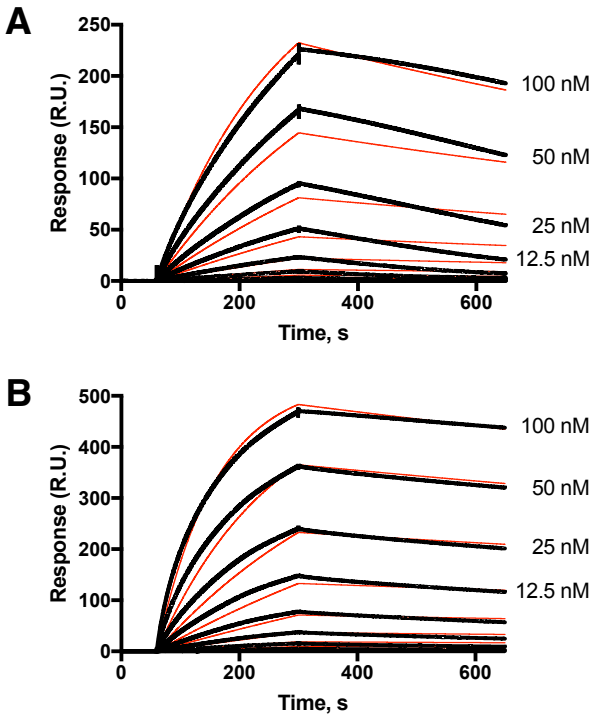

CS-E	
k_{on}	4.29 x 10^4 M^{-1} s^{-1}
k_{off}	6.31 x 10^{-4} s^{-1}
K_D	14.7 nM

HS	
k_{on}	9.60 x 10^4 M^{-1} s^{-1}
k_{off}	3.01 x 10^{-4} s^{-1}
K_D	3.14 nM

Figure 3-5. Carbohydrate surface plasmon resonance to examine kinetics of Tie1-GAG binding. Biotinylated (A) CS-E or (B) HS were immobilized onto a CM5 sensor chip, and Tie1-Fc was flowed over at different concentrations. Kinetic parameters were obtained by fitting to a one-to-one Langmuir binding model.

We next assessed the sulfation specificity of the Tie1-GAG interactions using carbohydrate microarrays.[33] Tie1- and Tie2-Fc conjugates were incubated on glass slides with different CS and HS epitopes electrostatically immobilized on the surface. Bound proteins were detected using a fluorescently tagged anti-human Fc antibody. As expected, Tie1 showed robust binding with the CS-E (Figure 3-4a) and HS (Figure 3-4b) epitopes with minimal binding to all other sulfation patterns.

Finally, we further quantified the Tie1-GAG interactions using surface plasmon resonance (SPR) analysis.[38] In this experiment, SPR CM5 sensor chips

covalently modified with carboxymethylated dextran were functionalized with streptavidin to allow for immobilization of biotinylated CS-E or HS. Solutions of Tie1-Fc at different concentrations were then flowed over the modified chip followed by buffer only, and the response rate was measured over time. We were pleased to see that both CS-E (Figure 3-5a) and HS (Figure 3-5b) gave dissociation constants that were similar to those observed via ELISA (CS-E: 14.7 nM; HS: 3.16 nM). Both carbohydrates also demonstrated similar binding kinetics with k_{off} values around 10^{-4} s^{-1}, suggesting a theoretical half-life for the complexes of roughly 18 min (CS-E) and 38 min (HS). These off rates are smaller than those reported for known hep/HS binding proteins VEGFR1 and neuropilin 1 (Nrp1),[37] implicating the physiological relevance of these binding events in vascular tissue.

3.2.2 Identification of the Tie1-GAG Binding Site

Having shown that Tie1 binds to GAGs through numerous methods, we aimed to decipher the exact location of the Tie1-GAG binding site to help provide structural clues on the importance of these novel interactions. No known consensus primary sequence or secondary structure has been found as a predictive measure for GAG-protein binding. As expected, GAG binding in many cases requires numerous surface-exposed positively charged Arg and Lys residues, which can occur on any number of domain structures. Tie1 contains both immunoglobulin-like (Ig) domains, which interact with hep/HS in FGFR1,[27] and fibronectin type III (FNIII) domains, which bind to CS-E in EphA4 and -B3 receptors.[39, 40]

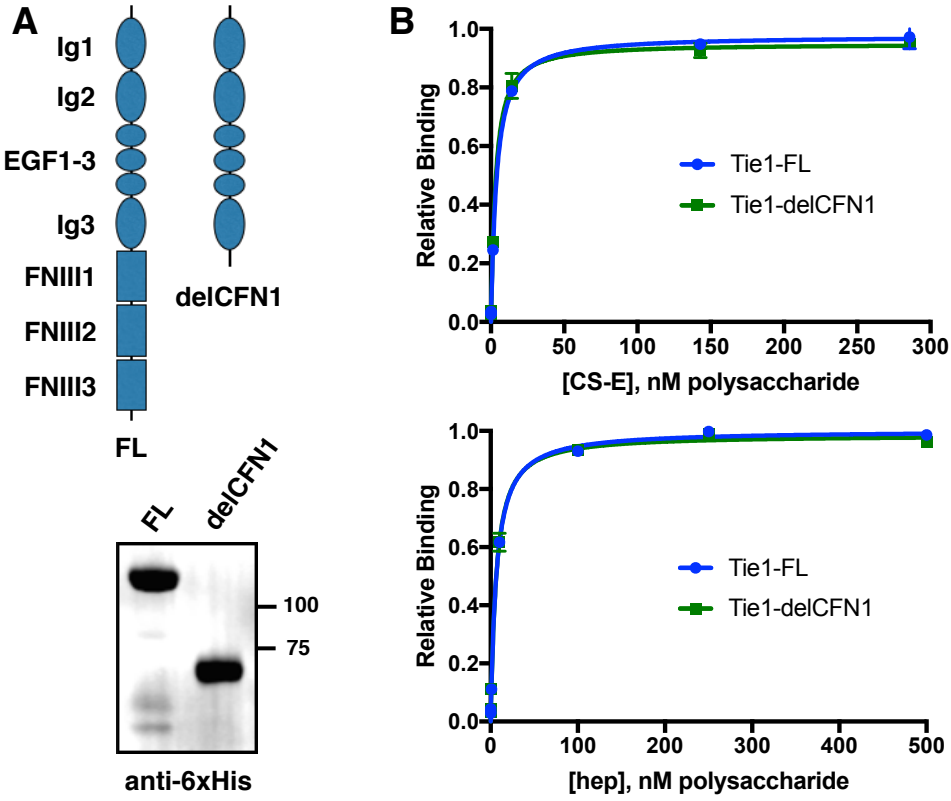

Figure 3-6. Tie1 truncations to determine Tie1-GAG binding domain. (A) Full length (FL) and truncated (delCFN1) Tie1-Fc were expressed and purified. (B) Expressed Tie1-Fc constructs were used in carbohydrate ELISA as described earlier. Both constructs maintain binding to GAGs, suggesting that binding occurs in the *N*-terminal domains of Tie1.

As a first step, we produced Tie1-Fc conjugates that contained, the full-length ectodomain (Tie1-FL-Fc) or a *C*-terminal truncation that eliminated the three FNIII domains (Tie1-delCFN-Fc). The two constructs were expressed as secreted proteins and purified by immobilized metal affinity chromatography (IMAC) using a *C*-terminal 6xHis tag (Figure 3-6a). These constructs were then used in the ELISA format described above. We found that both constructs showed binding with CS-E and HS, suggesting that the Tie1-GAG binding site was contained within the *N*-terminal Ig1/2 or EGF1-3 domains (Figure 3-6b). We

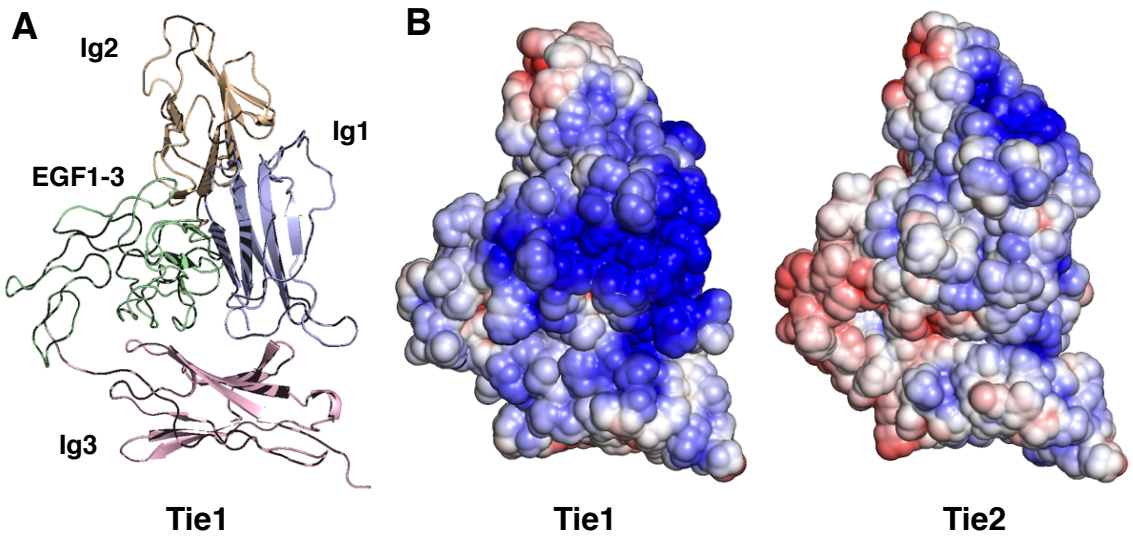

Figure 3-7. Homology model of Tie1. (A) Ribbon structure of Tie1 homology model built by SWISS-MODEL using Tie2 crystal structure. (B) Surface electrostatic potential maps of Tie1 and Tie2.

tried to express complementary *N*-terminal truncations of the protein, but none of these constructs expressed at high enough quantities to be used in the ELISA. This result is likely due to the predicted globular structure formed by the *N*-terminal domains in the final folded protein.

Because we could not isolate the Tie1-GAG binding site further by truncation, we turned to computational docking of GAG structures with Tie1 to predict key residues for the interaction.[33] This approach has been successfully used to define likely regions of GAG binding on a number of proteins, including the malarial protein VAR2CSA, tumor necrosis factor α (TNFα), and Ephs A4 and B3.[33, 39, 40] To conduct docking, we first produced a homology model of Tie1 based on the solved Tie2 crystal structure[41] using the SWISS-MODEL program (Figure 3-7a).[42]

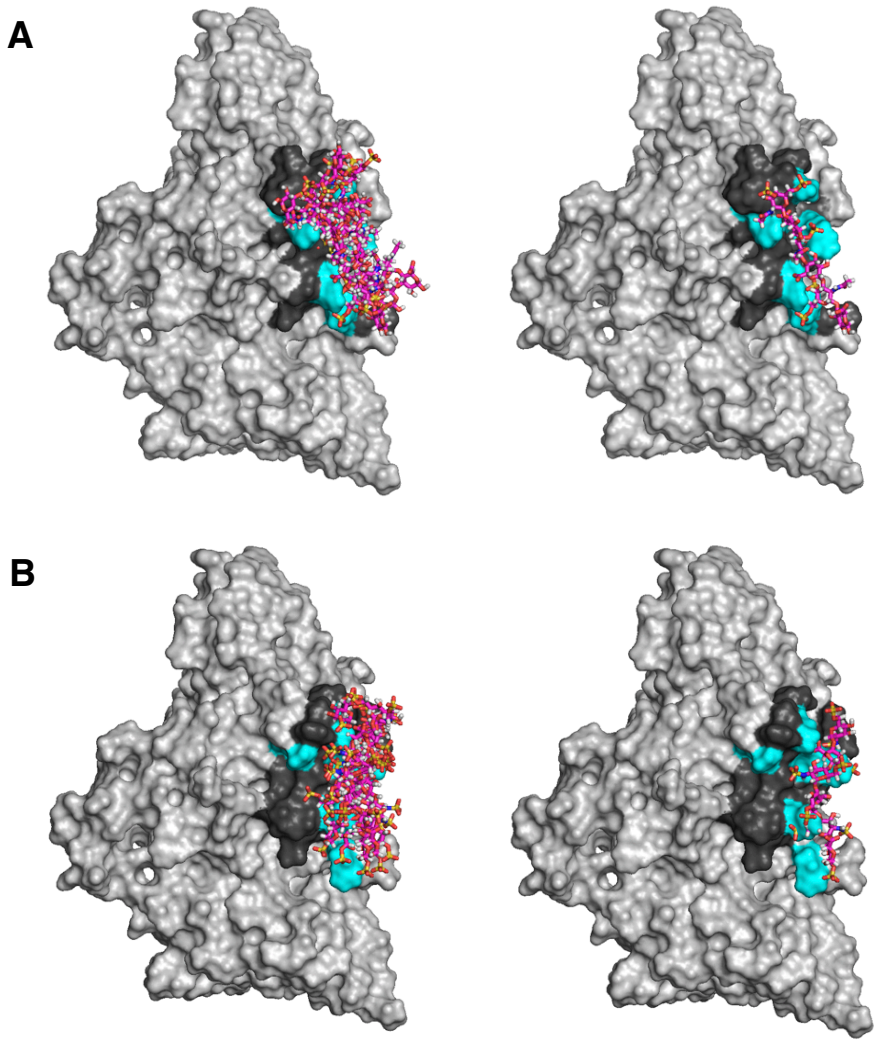

Figure 3-8. Docking of CS-E and HS hexasaccharides to Tie1. Top 10 and top 1 binding poses of (A) CS-E and (B) HS onto the Tie1 homology model.

Tie2 shares the same domain structure as Tie1 along with 39% total amino acid identity. Upon inspection of the electrostatic potential maps of the Tie1 and Tie2 structures (Figure 3-7b), the Tie1 model displays a large electropositive region encompassing parts of the Ig1 and three EGF domains. This electropositivity is severely attenuated in the Tie2 structure, providing evidence for the specificity of

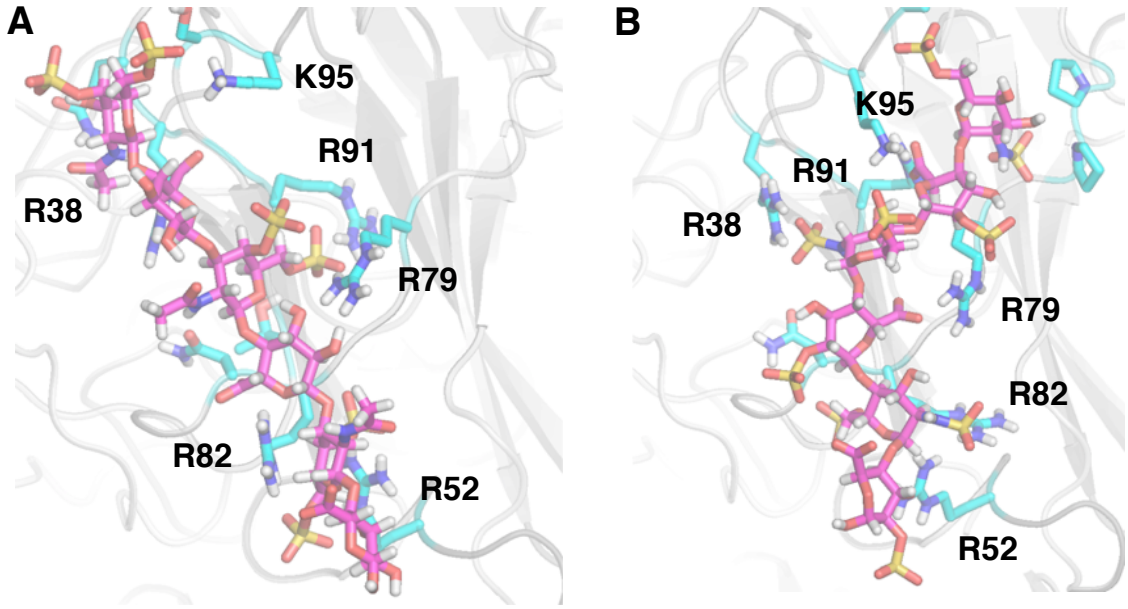

Figure 3-9. Amino acids in putative GAG binding site of Tie1. Positively charged amino acids surrounding the top binding pose for (A) CS-E and (B) HS.

GAG binding to Tie1. Interestingly, this region of Tie1 had previously been suggested to interact with a complementary electronegative face of Tie2.[25]

With a model for Tie1 in hand, we then docked hexasaccharide structures of CS-E and HS to the predicted structure and ranked poses based on the calculated binding energies. The top 10 poses of both CS-E and HS clustered in one portion of the large electropositive region centered on the Ig1 domain (Figure 3-8). Upon closer inspection, the top ranked pose of both docked GAG structures showed close association with six positively charged residues: Arg-38, Arg-52, Arg-79, Arg-82, Arg-91, and Arg-95 (Figure 3-9). Using genomic alignment, we found that four of these six residues (Arg-38, Arg-52, Arg-82, Arg-91) were highly conserved

Figure 3-10. Sequence alignment of *N*-terminal Tie1 gene. Predicted binding site amino acids are bolded with conserved amino acids highlighted.

throughout all mammals (Figure 3-10), with Lys-95 showing moderate conservation as well.

We turned to the ELISA format to test the accuracy of our computational predictions. Wild-type Tie1-Fc (Tie1-WT) along with a mutant containing all six residues mutated to Ala (Tie1-6A) and a second mutant containing R38A and R82A (Tie1-2A) were cloned and expressed using the secretion system previously described. Importantly, both mutants expressed well, suggesting that the mutations did not affect protein folding as seen for the *N*-terminal truncations. We were pleased to see that binding of both biotinylated CS-E and HS was severely attenuated after mutation (Figure 3-11), confirming that these residues were critical for the Tie1-GAG interaction. We attempted the same experiment using single mutations, but neither showed complete loss of Tie1

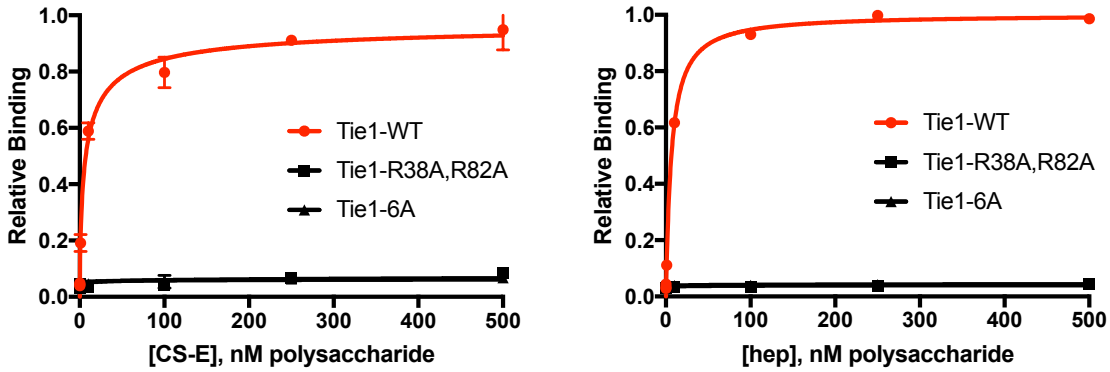

Figure 3-11. Carbohydrate ELISA of Tie1 mutant constructs. FL, wild-type (WT), 6A, and 2A mutants were expressed, purified, and used in carbohydrate ELISA binding assays as previously described. Both mutant constructs completely lost binding to GAGs, corroborating the computational results.

binding, suggesting that the double mutation was the minimal perturbation necessary to disrupt the Tie1-GAG interaction.

3.2.3 Contextualization of Tie1-GAG Binding

Although up to this point we had tested Tie1 binding to GAGs using both CS-E and HS, we desired to establish which GAG structures would be the most relevant for *in vivo* binding. Tie1 is expressed universally on endothelial cells during late development,[43] after which expression levels are strongly downregulated in the adult except in a small subset of remodeling endothelial cells.[22] Tie1 expression is also stimulated during angiogenic processes such as wound healing and tumor formation and regions of nonlaminar flow like branch points of vessels.[17, 18] Therefore, examining the GAGs produced by endothelial cell lines would provide helpful information to decipher the relative importance of CS-E and HS in Tie1 binding.

Previously, methods to quantify the absolute amounts of different GAG sulfation patterns on the cell surface, termed glycosaminoglycanomics, have found that human umbilical vein endothelial cells (HUVECs) are dominated by HS.[44] In fact, HUVECs, which are used as a model system for systemic endothelial cells, were found to contain the highest proportion of HS and the HS epitope out of all cell lines tested. HS was found at nearly a 10:1 w/w ratio compared to CS. Moreover, CS-E was not detected in HUVECs in this analysis, strongly suggesting that HS was the physiologically relevant GAG for Tie1 binding at least in systemic endothelial cells.

We confirmed these finding using a cell binding assay (Figure 3-12). HUVECs were grown to confluency, treated with or without a mixture of heparinase I and III and fixed. Cells were then incubated with Tie1-WT-Fc or Tie1-2A-Fc, and binding of the constructs was detected using a fluorescently tagged anti-human Fc antibody. Importantly, we saw that Tie1-WT binding was significantly decreased after treatment of the cells with heparinase I/III, with all remaining Tie1-WT staining colocalizing with residual HS signal as detected by an anti-HS antibody. Moreover, binding of Tie1-2A was not observed even with cell surface HS intact. Together, these results suggest that cell surface HS is necessary for Tie1 binding through the predicted Tie1-GAG binding interface and that loss of cell surface HS or the residues necessary for this interaction is sufficient to prevent Tie1 binding.

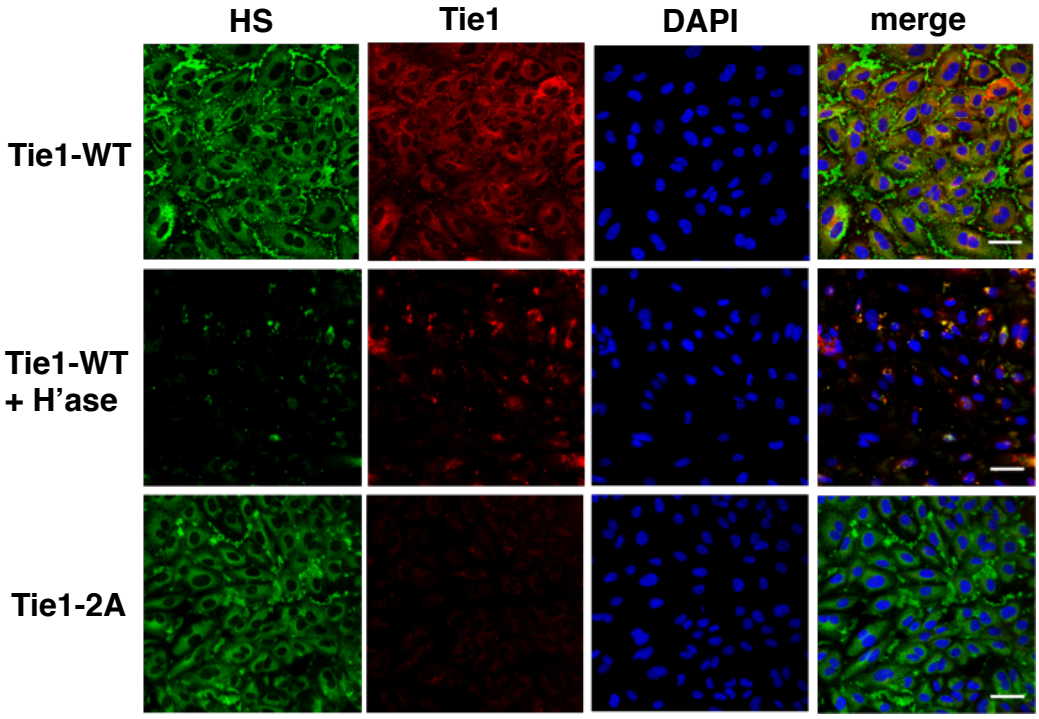

Figure 3-12. HS-dependent Tie1 binding to endothelial cells. Untreated or heparinase-treated EA.hy926 cells were probed with Tie1-WT and visualized with an anti-human Fc antibody (red). In parallel, cells were probed using an anti-HS antibody (green) and DAPI (blue). Robust binding was observed for untreated cells, which was lost upon heparinase treatment. Tie1-2A showed no binding to cells, suggesting that binding to HS is necessary to cell surface binding.

3.2.4 Towards a Functional Role of Tie-GAG Binding

To further characterize the importance of the Tie1-HS binding interaction, we turned to cellular assays. Unfortunately, Tie1 presents a number of unique challenges to understand its functional role. For example, the most common method to examine the functional output of an RTK is through phosphorylation assays.[45] Although Tie1 contains an intracellular tyrosine kinase domain, evidence of Tie1 homodimeric activation and cross-phosphorylation has not been observed as seen for other RTKs,[46, 47] precluding a commonly used, facile readout for RTK

activity. Early reports using chimeric proteins containing the intracellular Tie1 kinase domain fused to extracellular domain of either tropomyosin-related kinase A (TrkA) or colony stimulating factor 1 (c-fms) receptor provided conflicting results over whether "forced" homodimerization by stimulation with the canonical ligands of TrkA or c-fms could induce cross-phosphorylation,[48, 49] further obfuscating the relevance of Tie1 kinase activity. Conversely, Tie2 activation by angiopoietin ligands can lead to Tie1 phosphorylation through heterodimerization;[46, 47] however, this approach introduces additional HS-binding partners to the experiment (see Section 3.4), preventing the straightforward delineation of the role of HS binding on one protein within the larger system.

To circumvent these concerns, we focused on examining the transient association of Tie1 with other cell surface receptors. The Tie1/Tie2 heterodimer has been documented previously and is the basis of Tie2-induced phosphorylation of Tie1;[46, 47] however, this interaction has been observed using standard co-immunoprecipitation techniques. Instead, cross-linking of surface receptors has been used to preserve the interaction for co-immunoprecipitation.[46, 50, 51] More recently, integrin $\alpha_5\beta_1$ has also been implicated to associate with Tie1 and Tie2 at the cell surface,[51] and its removal prevents Tie2 signaling.[26] As proof of principle, we used the immortalized endothelial cell line EA.hy926 and treated the cells with the cell-impermeable cross-linking agent 3,3'-dithiobis(sulfosuccinimidyl propionate) (DTSSP). Cells were then lysed and immunoprecipitated for Tie1. Cells treated with DTSSP showed robust co-immunoprecipitation of Tie2 as well

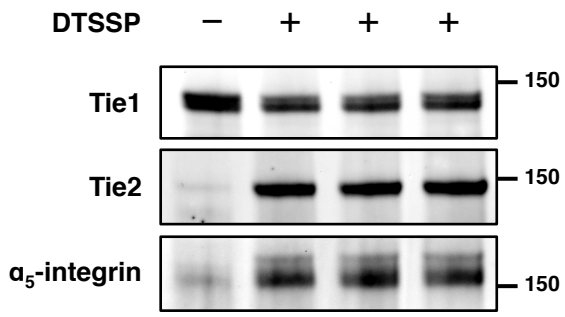

Figure 3-13. Tie1 association with Tie2 and α_5-integrin. EA.hy926 cells were treated with cross-linker DTSSP, lysed, and immunoprecipitated for Tie1. Samples were analyzed by Western blotting.

as integrin α_5 (Figure 3-13). In the near future, we plan to expand this assay out with heparinase treatment and cell surface glycan engineering (see Section 3.4.3).

As an alternative approach to observe Tie1/Tie2 heterodimers, we have also employed proximity ligation assays (PLA).[52] This assay is similar in format to standard immunocytochemistry (ICC) techniques where two proteins are probed for with separate primary antibodies. The method diverges from ICC in that the secondary antibodies are modified with single stranded DNA oligonucleotides rather than fluorescent dyes. Through subsequent annealing and ligation steps, a substrate is formed for rolling circle amplification, at which point fluorescently labeled nucleotides are incorporated into the growing DNA strand. These fluorescent oligonucleotides can then be detected by standard immunofluorescence imaging. Importantly, this procedure will produce punctate staining only at locations where both primary antibodies bound, providing a signal only where the two target proteins are in close proximity with one another. We optimized this assay for the Tie1/Tie2 heterocomplex using two antibodies

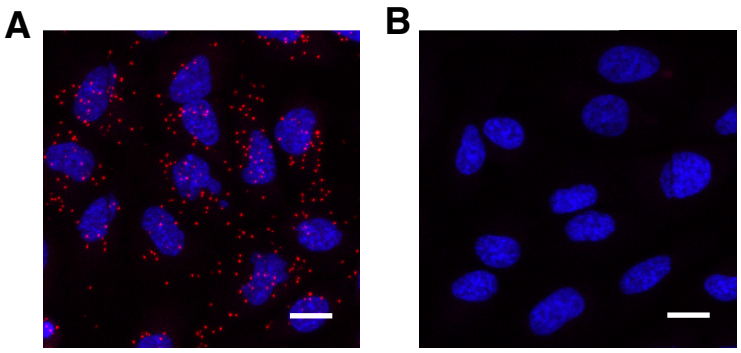

Figure 3-14. Direct observation of Tie1/Tie2 heterocomplexes by PLA. EA.hy926 cells were fixed, immunostained with (A) anti-Tie1 and anti-Tie2 antibodies or (B) anti-Tie1 antibody alone, stained with the PLA staining protocol, and visualized by microscopy. Tie1/Tie2 heterocomplexes are revealed as punctate red staining and can be normalized to cell count by DAPI (blue) nuclear staining. Scale bar = 20 μm.

specific for the extracellular domains of each protein (Figure 3-14). Briefly, HUVECs or EA.hy926 cells were fixed, blocked, and probed with the appropriate Tie1 and Tie2 antibodies. Cells were then subjected to PLA procedures according to the manufacturer's specifications. Cells were then co-stained with DAPI and visualized by confocal microscopy. We were pleased to observe the formation of punctate staining at the cell surface when both antibodies were used, whereas a control sample lacking one of the two primary antibodies showed minimal background. As before, we will apply both heparinase and glycan engineering techniques to this assay to further delineate the effect of HS on Tie1/Tie2 heterodimerization.

3.2.5 Generation of a Tie1-GAG-Binding Deficient Mouse Model

Further examination of the Tie1-GAG binding event requires the use of functional systems. Here again, the Tie/Ang signaling axis provides a number of

unique challenges. Unlike many other functional outcomes of RTKs such as growth promotion or inhibition, the outcomes of the Tie/Ang pathway such as vessel development, maturation, and remodeling are not easily testable *in vitro*. The closest related *in vitro* assay, measuring apoptosis in response to serum and growth factor starvation, has been used infrequently with angiopoietin ligand stimulation;[53] however, very few other reported *in vitro* assays exist that can directly examine the formation and maintenance of vascular tissue. Instead, many researchers have turned to *in vivo* models to test Tie/Ang function.

The lethality of constitutive Tie1 and Tie2 knockout models prevented further examination of Tie1/2 function in adult animals.[11-13] This led to the development of floxed Tie1 animals crossed with mice expressing cre recombinase under endothelial-specific, tamoxifen-dependent promoters (such as the *Cdh5-creERT2* and *Tal1/SCL-creERT* lines) to provide adult mice with endothelial-specific Tie1 knockout.[17, 26] Although these mice have been invaluable for the study of Tie1 function *in vivo*, they do not provide a straightforward way to ascertain the importance of the Tie1-GAG interaction specifically. Similarly, a number of different HS biosynthesis conditional knockout animals exist, with Ndst1 being commonly used since animals have much lower HS sulfation in the targeted tissue.[54, 55] However, these models also suffer from questions of specificity for our purposes. HS binds to a number of angiogenic ligands and receptors; thus, understanding the ramifications of the Tie1-GAG interaction caused by a global decrease in overall HS sulfation (and thereby overall HS/protein binding) may be

also difficult to parse. Therefore, we turned our attention to a mouse model that could specifically disrupt the Tie1-GAG interaction using insights gained from mutational studies.

To achieve this selective mouse model, we chose to pursue a novel approach using gene editing with the clustered regularly interspaced short palindromic repeats (CRISPR)/Cas9 platform.[56-58] Here, the Cas9 nuclease protein is directed to specific regions of the genome by a complementary single stranded RNA sequence known as a guide RNA (gRNA). Once localized to the sequence, Cas9 induces a double strand break within the complementary genomic DNA (gDNA) sequence. In the absence of a repair template, endogenous machinery of the cell undergoes non-homologous end joining (NHEJ), thereby producing random insertions and deletions (indels). Alternatively, a repair template is added along with the gRNAs and Cas9. Here, homology-directed repair (HDR) machinery can compete with NHEJ to incorporate the repair template at the DSB site. This approach has been used successfully to incorporate a variety of site mutations, small reporter tags, and fluorescent protein fusions onto endogenously expressed proteins.[59] Importantly, this approach provides a number of benefits compared to other methods like lentiviral delivery or transient expression in that the incorporation event is highly controlled and will not interrupt other genes at random, expression levels will be controlled by the endogenous promoter and subjected to native regulation, and endogenous proteins do not need to be silenced to replace with a mutated sequence. Furthermore, CRISPR/Cas9

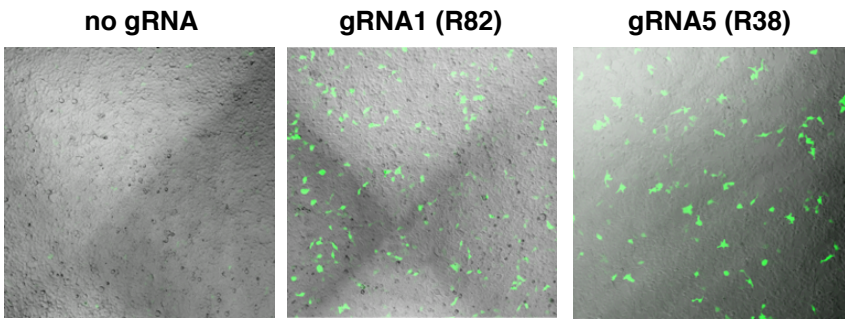

Figure 3-15. Validation of guide RNAs in HEK-293T cells. HEK-293T cells were transfected with the pCAG-EG(Tie1)FP plasmid plus empty pX459 (no gRNA) or pX459 containing gRNA1 or gRNA5. gRNA targeting efficiency was measured by the formation of GFP^+ cells.

transgenic animal production does not require the extensive screening of stem cell clones like previous transgenic methods.[60] Finally, we believe that this approach will be a powerful new tool for glycobiology, allowing a clear-cut method to understand the importance of a single GAG-receptor binding event without globally affecting other carbohydrate-protein interactions.

We decided to target the R38A and R82A mutations for genomic incorporation. The efficiency of mutation incorporation by HDR decreases rapidly more than 10-20 base pairs (bp) away from the DSB site.[61] Because the codons for these residues are roughly 130 bp away from one another, we decided to use a dual gRNA approach that would cut near each of the targeted mutation sites. gRNAs were designed using the online CHOPCHOP computational tool for the sequences flanking each codon, and four to five gRNAs for each region were selected based on predicted cutting efficiency and minimal off-target homology. These gRNAs were cloned into pX459 gRNA/Cas9 vector to test their cutting efficiency. We chose to use a recently described activity assay for gRNA

screening in which the genomic region of interest is cloned within a broken GFP construct (pCAG-EGxxFP).[62] If cut, the vector undergoes self-mediated HDR using homology regions of GFP flanking the inserted gDNA sequence to produce a functional GFP construct. The Tie1 genomic region of interest was amplified from murine gDNA and inserted into the pCAG-EGxxFP construct to produce pCAG-EG(Tie1)FP. pX459 vectors containing each gRNA and pCAG-EG(Tie1)FP were co-transfected into human embryonic kidney (HEK) 293T cells, which were then visualized after 48 h (Figure 3-15). gRNAs that produced the highest percentage of GFP^+ cells were chosen for *in vivo* experiments.

Next, the repair template was designed. Two types of repair templates have been used previously: single stranded oligonucleotides (ssODNs) or double stranded DNA (dsDNA).[59] ssODNs generally are upwards of 200 nucleotides (nt) in length, with roughly 60 nt of homologous sequence on either side of the inserted sequence. Conversely, dsDNA templates are less effective for HDR and require hundreds of bp of homologous sequence for efficient incorporation. Because we aimed to incorporate mutations roughly 130 bp apart, we tried both approaches. Two ssODN constructs were produced containing one of the two mutations flanked by roughly 60 nt of homologous sequence. The dsDNA construct was designed to contain the same central 130-bp sequence flanked by roughly 550 bp of homologous sequence. Within the region surrounding the Arg-38 and Arg-82 codons, a number of mutations were made. First, the two codons were mutated to Ala codons. Second, a silent mutation was incorporated into the

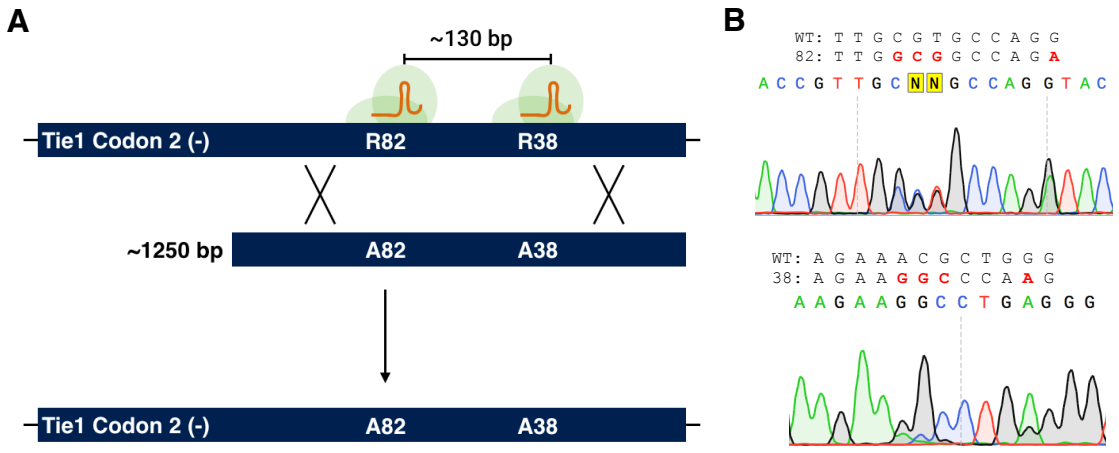

Figure 3-16. CRISPR/Cas9-mediated *in vivo* Tie1 mutations. (A) Schematic of CRISPR/Cas9 strategy to introduce R38A and R82A mutations *in vivo*. Two gRNAs specific to regions around each codon of interest along with a dsDNA donor will be used to introduce the mutations. (B) Sequencing results from successful heterozygous mutations in B6SJL-F1/J blastocysts.

protospacer motif (PAM) for each gRNA. Cas9 recognition of gDNA requires an NGG motif known as the PAM immediately at the 3'-end of the gRNA complementary sequence. Loss of the NGG seqeunce prevents Cas9 from cutting the sequence again after the mutation has been incorporated. Finally, silent mutations were added at each site to incorporate restriction enzyme cut sites to allow for facile genotyping. Both the ssODN and ssDNA constructs were commercially purchased along with the gRNA sequence and Cas9 protein.

To test efficiency *in vivo*, the two gRNA/Cas9 complexes were formed *in vitro* and pronuclearly injected into fertilized B6SJL-F1/J murine zygotes at 20 ng/μL each along with either the pair of ssODNs or dsDNA construct at 20 or 10 ng/μL, respectively, in 10 mM Tris pH 8.0, 1 mM EDTA. B6SJL-F1/J mice (the F1 generation crossing of a C57BL/6 female and a SJL/J male) were chosen because

of their relatively large litter sizes and hybrid vigor compared to inbred lines. Zygotes were allowed to develop to the blastocyst phase, at which point they were subjected to genotyping to test for incorporation of the desired mutations. Genotyping was achieved by harvesting gDNA from the blastocysts followed by PCR amplification of the desired sequence and Sanger sequencing (Figure 3-16). In both cases, the majority of the zygotes proceeded to the blastocyst stage (ssODN: 15/18; dsDNA: 15/21), suggesting that the injection solutions were nontoxic. Interestingly, sequencing results showed that the majority of the blastocysts resulting from ssODN injection showed random indels, with no sample showing proper incorporation. This was unexpected as ssODN repair templates had previously been described as highly efficient. We were happy to see that 4/15 blastocysts from dsDNA injection showed proper incorporation of the mutations at both of the sites (Figure 3-16b). We chose this method to proceed to large-scale injection and implantation.

For large-scale injection and implantation, roughly 80 fertilized zygotes were harvested from the oviducts of superovulated, mated B6SJL/J mice, injected with the gRNA/Cas9/dsDNA mixture described above, allowed to mature to the blastocyst stage, and then implanted at ~20 zygotes per surrogate mother. This was repeated three times, which resulted in seven litters containing 19 total pups. The litter sizes were small, but this is expected since loss of Tie1, which could be caused by indels from competing NHEJ processes, is embryonic lethal. Unfortunately, none of the animals possessed the desired genotype. The

experiment was repeated using a higher concentration of dsDNA (20 ng/μL) and incubation of the zygotes with the NHEJ inhibitor SCR7.[63] Here, four litters containing a total of 15 pups were obtained. Excitingly, three pups were heterozygous for the desired mutations, with the other Tie1 allele containing small in-frame deletions. Two of the pups were produced from zygotes incubated with SCR7, whereas one was derived from untreated zygotes. The SCR7-treated pups contained 6- and 9-bp deletions, and the untreated pup contained a larger in-frame deletion of 90 bp, providing anecdotal evidence of the efficacy of SCR7 in inhibiting at least large NHEJ events. The now adult mice are currently set up in breeding pairs with C57BL/6 mice to expand the colony for future homozygous crossing and phenotypic analysis.

3.3 HS GAGs Bind to Angiopoietin Ligands and Potentiate Tie2 Signaling

3.3.1 ELISA

In addition to the Tie receptors, we also examined whether the related angiopoietin ligands Ang1, -2, and -4 could also interact with HS. Previously, Ang1 but not Ang2 has been shown to associate with the extracellular matrix (ECM) via its linker peptide region;[64] however, the purified Ang1 constructs used therein did not bind to heparin or soluble Tie2-Fc. In a separate report, Ang3, the functionally distinct murine ortholog to human Ang4, was shown to be anchored to the extracellular matrix through HSPGs like perlecan,[65] raising the possibility of Ang4 association with HS. To test binding, we used a modified version of the

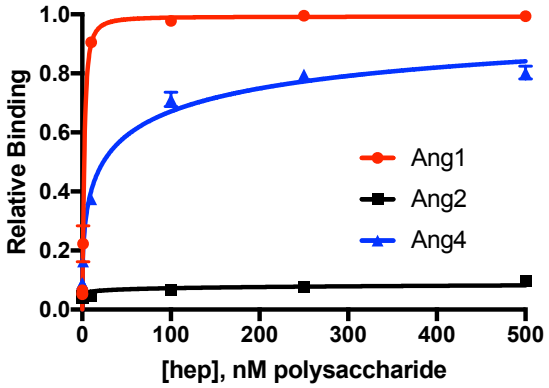

Figure 3-17. Carbohydrate ELISA using angiopoietin ligands. Ang-6xHis constructs immobilized on Cu plates were probed with biotinylated HS as previously described. Ang1 and Ang4 show nanomolar affinity to HS, whereas Ang2 does not bind.

carbohydrate ELISA platform. Ang constructs containing a *C*-terminal 6xHis tag were immobilized onto copper functionalized plates and incubated with biotinylated HS. Here, Ang1 and Ang4 showed strong binding to HS, with dissociation constants of 2.23 ± 0.27 nM and 42.0 ± 43.0 nM, respectively, whereas Ang2 did not show binding to HS (Figure 3-17). The strong affinity of Ang1 for HS is in direct conflict with results described from previous experiments.[64] However, the constructs used in the previous paper were over-expressed in murine cancer cell lines LLC and TA3 and the simian kidney cell line Cos7, which may have produced misfolded forms of the protein.

3.3.2 Ternary Complex Formation with Tie2

GAGs have been shown previously to both facilitate and impede the formation of a ligand-receptor interaction,[33] thus exerting control over receptor activation and signaling. To rapidly delineate whether HS binding to Ang1 or Ang4 affects their binding to Tie2, we employed carbohydrate microarrays to directly observe

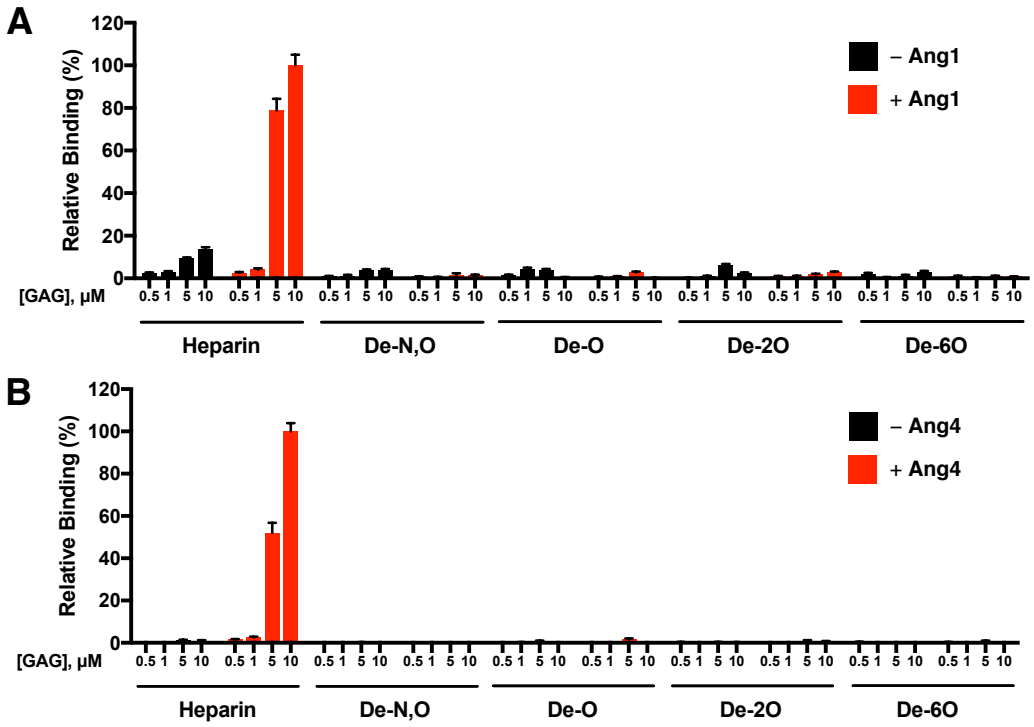

Figure 3-18. Ternary complex formation of Tie2-Ang-HS. HS carbohydrate microarrays were incubated with Tie2-Fc with or without (A) Ang1 or (B) Ang4. Immobilized Tie2-Fc was visualized using an anti-human Fc antibody. Binding of Tie2-Fc to the microarray in the presence of Ang1 or Ang4 suggests the formation of carbohydrate-protein-protein ternary complexes.

the formation of ternary, carbohydrate-protein-protein interactions (Figure 3-18). Here, Tie2-Fc, which was previously shown not to bind HS, was incubated with the HS microarrays in the presence or absence of Ang1 or Ang4. Tie2 immobilized onto the microarray through its interaction with HS-bound Ang1/4 was visualized by a fluorescently tagged anti-human Fc antibody. As previously shown, signal from Tie2 alone was not observed on the HS microarray. Interestingly, Tie2 signal dramatically increased in the presence of either Ang1 or Ang4, suggesting that the Ang/HS interaction does not interfere with Ang/Tie2

binding and that the three biomolecules can exist as a single ternary complex. Moreover, the assembly of this ternary complex is sulfation pattern dependent, forming only with the HS motif. This mode of ternary complex formation has previously been demonstrated for both FGF2-FGFR1 and FGF8-FGFR3[66] and suggests that HS at the cell surface can potentiate Ang/Tie2 signaling by bringing Ang ligands into close proximity with the Tie2 receptor.

3.3.3 Potentiation of Tie2 Signaling by Glycan Engineering

To examine whether cell surface HS could affect Ang/Tie2 signaling, we decided to utilize our HTP glycan engineering technique.[66] Endothelial cells are generally very refractory to transient transfection;[67] therefore, a lentiviral delivery approach was developed. Here, the HTP transmembrane construct was cloned into a pENTR4 vector and transferred to a pLenti-CMV-Blast destination vector using Gateway cloning.[68] Lentiviruses (HTP-LV) were produced using third generation packaging plasmids in HEK-293T cells and concentrated by PEG precipitation.[69] The endothelial EA.hy926 cell line was treated with different amounts of HTP-LV and subjected to selection with blasticidin after 48 h. Cells from the sample treated with the lowest amount of HTP-LV that survived three days after all untreated cells were killed were used as the EA.hy926-HTP cell line moving forward. To validate the expression of HTP on the cell surface, EA.hy926-HTP and untransduced, parental cells were treated with cell-impermeable AF488-CL and Hoescht 33324 dye for 15 min at 37 °C, washed, and live imaged (Figure

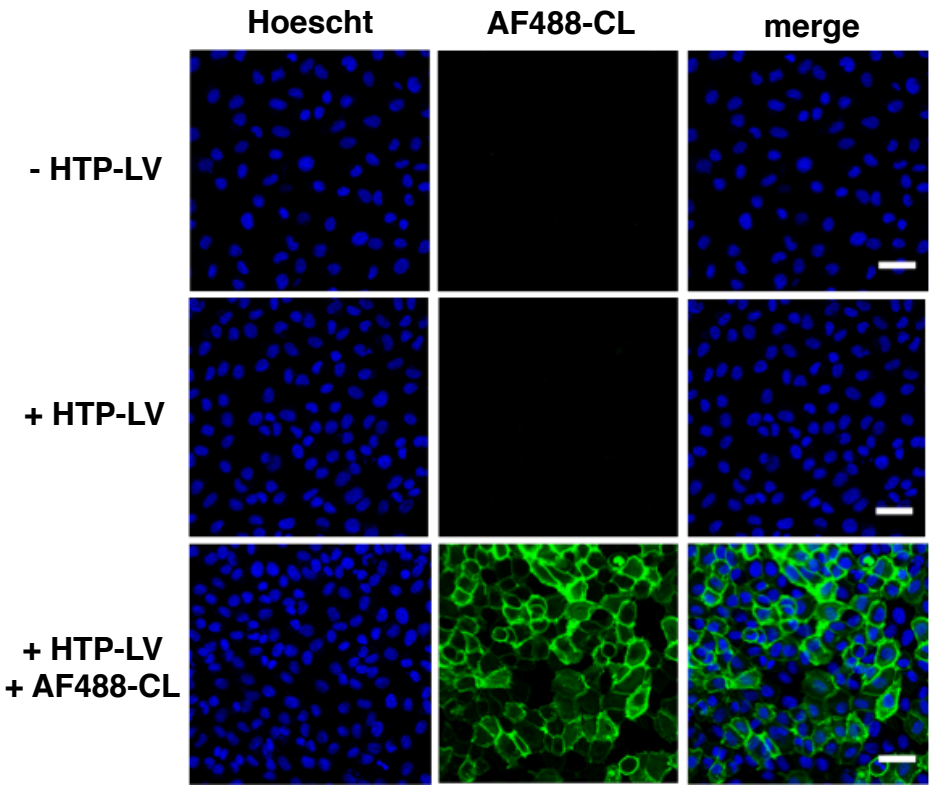

Figure 3-19. Production of an HTP-expressing endothelial cell line. EA.hy926 cells were treated with an HTP-expressing lentivirus and selected for incorporation. The resulting cells (+ HTP-LV) and the parental cells (- HTP-LV) were treated with AF488-CL to visualize cell-surface HTP. Scale bar = 50 μm.

3-19). As expected, cells treated with HTP-LV showed robust surface labeling by AF488-CL, whereas the parental cells showed no surface labeling.

With HTP-expressing endothelial cells in hand, we set to test the effect of cell-surface HS on Ang/Tie2 signaling (Figure 3-20). To achieve this, EA.hy926-HTP cells were first treated with heparinase I/III to eliminate endogenous HS and then grown to confluency. Cells then treated with either 5 μg/mL HS-CL or desulfated (deS) HS-CL for 2 h at 37 °C in serum-starved medium (0.5% fetal bovine serum). Cells were washed and then incubated for another 4 h in serum-starved medium

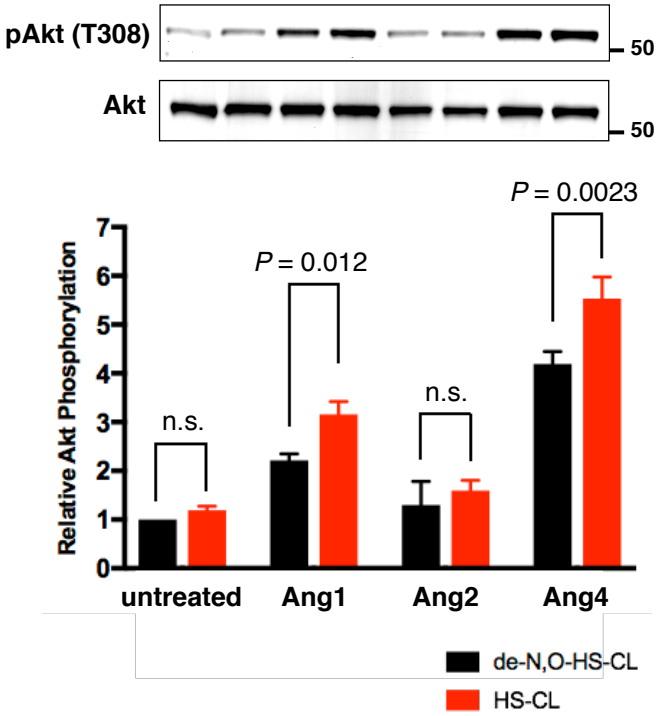

Figure 3-20. Potentiation of Tie2 signaling by glycan engineering. EA.hy926 cells expressing HTP were treated with de-HS-CL or HS-CL and stimulated with Ang1, Ang2, or Ang4. Tie2 activation was quantified by measurement of Akt phosphorylation at Thr-308 using Western blotting.

and then treated with 500 ng/mL Ang1, Ang2, or Ang4 for 30 min at 37 °C. Cells were then washed with PBS and immediately lysed. Phosphorylation of Akt at Thr308, which is dependent on 3-phosphoinositide dependent kinase 1 (PDK1), was then measured by Western blotting as a readout for downstream Tie2 signaling. Impressively, we saw that for both Ang1 and Ang4, the presence of HS-CL on the cell surface led to a significant increase in Akt phosphorylation compared to cells displaying with the non-binding de-HS-CL. No significant difference was observed at basal levels or with Ang2, suggesting that this effect is specific to increased Tie2 activation by Ang1 and Ang4 bound to HS. Together with the ternary complexation data, these results suggest that HS, which is highly

upregulated at the cell surface of endothelial cells, can potentiate Tie2 activation by Ang1 and Ang4 through the formation of active ternary signaling complexes.

3.4 Conclusions

The results presented herein provide the first evidence for the involvement of HS in the Ang/Tie signaling pathway. The binding of orphan receptor Tie1 to GAGs is the first report of a ligand for this protein since its discovery 25 years ago. Furthermore, the use of biochemical and chemical biology tools to identify amino acid residues necessary for the Tie1-GAG interaction has allowed the production of an animal model that is deficient in this interaction without removing the protein or the carbohydrate. This is the first report of an animal model using this approach, which will provide unparalleled, specific information of the importance of a protein-carbohydrate interaction *in vivo*. Moreover, the interaction between HS and Ang1 and Ang4 parallel the widely observed phenomenon of HS-ligand interactions. Using our glycan engineering method, we were able to provide direct evidence that HS on the cell surface potentiates signaling through HS-Ang1/4-Tie2 ternary complexes as demonstrated by our carbohydrate microarrays. These results as a whole provide crucial information regarding the regulation of the Tie/Ang signaling axis and may help further delineate the molecular mechanisms of a well-known but poorly understood RTK subfamily.

3.5 Methods and Materials

3.5.1 General Methods

Molecular biology. All reagents used for molecular biology were obtained from New England Biolabs unless otherwise noted. All primers were obtained from Integrated DNA Technologies. All miniprep, maxiprep, and gel extraction steps were conducted using Zymogen kits (Genesee Scientific). Cloning was generally achieved using the NEBuilder HiFi Cloning Master Mix (New England Biolabs). Human Tie1 cDNA was obtained from pDONR223-TIE1 plasmid (23946, Addgene) and cloned into a pCDNA3.1 vector (ThermoFisher Scientific) containing an *N*-terminal Ig κ-leader sequence and *C*-terminal human IgG_1 Fc and 6xHis tags. Truncations and site mutations were produced using the Q5 site-directed mutagenesis kit (New England Biolabs). The transmembrane HTP construct was produced as previously described.[66] To produce the lentiviral construct, he HTP sequence was first cloned into the pENTR4 vector (17424, Addgene) and then transferred into the pLenti-CMV-Blast vector (17451, Addgene) using the Gateway LR Clonase kit (ThermoFisher Scientific). Vectors used to test gRNA sequences include pCAG-EGxxFP (50716, Addgene) and pX459 (62988, Addgene).

Cell culture. All reagents used for cell culture were obtained from ThermoFisher Scientific unless otherwise noted. The EA.hy926 cell line, HEK-293T cell line and HUVECs were obtained from the American Type Culture Collection. EA.hy926 and HEK-293T cells were cultured in DMEM with 10% fetal bovine serum (FBS)

and 1x penicillin/streptomycin (P/S) (referred to now on as complete DMEM). HUVECs were cultured using endothelial cell basal medium (EBM-2, Lonza) with the EGM-2 Bulletkit additives (Lonza) (referred to now as EGM-2 medium) and were used for experiments between 0 and 5 passages. For serum starvation, EA.hy926 cells were cultured in DMEM with 0.5% FBS and 1x P/S. Cells were generally grown on plastic, tissue culture treated plates (Sarstedt) without any coating. For experiments, cells were plated onto plastic plates (for lysate harvesting) or glass-bottom plates (imaging) precoated with 5 $\mu g/cm^2$ bovine fibronectin (Sigma Aldrich) and 10 $\mu g/cm^2$ rat tail collagen type I (Sigma Aldrich). Plates were coated by incubation of plates with the above-mentioned proteins in sterile PBS for 1 h at 37 °C followed by two rinses with sterile PBS and were used immediately.

Western blotting. Protein samples were first diluted with one-fourth volume of 4x sodium dodecyl sulfate-polyacrylamine gel electrophoresis (SDS-PAGE) loading buffer (200 mM Tris pH 6.8, 400 mM DTT, 8% SDS, 40% glycerol, 0.4% bromophenol blue) and heated to 95 °C for 10 min. Samples were then loaded onto NuPAGE 4-12% Bis-Tris protein gels (NP0355BOX, ThermoFisher Scientific) and resolved using 180 V at RT for 1 h with constant voltage. The molecular weight of protein targets was estimated using Precision Plus Protein Dual Color Standards (Bio-Rad). Gels were then transferred onto Immobilion-FL PVDF membrane (IPFL00010, EMD Millipore) using 250 mA at 4 °C for 1-1.5 h with constant amperage. Membranes were then blocked for 1 h at RT with either

5% BSA in TBST (50 mM Tris pH 7.4, 150 mM NaCl, 0.1% Tween) for phosphoprotein detection, 1:1 Li-COR blocking buffer/TBS for goat primary antibodies, or with 5% nonfat milk in TBST, depending on the antibody specifications. In general, primary antibodies were used at 1:1000 (1 μg/mL) in the same buffer as the blocking step with incubation at 4 °C overnight with gentle rocking. Blots were rinsed thrice with TBST prior to incubation with secondary antibodies. In general, highly cross-adsorbed secondary antibodies containing AlexaFluor 680 or AlexaFluor 790 (ThermoFisher Scientific) were used at 1:10000 (0.2 μg/mL) in the same buffer as the blocking step with incubation at RT for 1 h with gentle rocking. Blots were then washed thrice for 5 min with TBST prior to imaging with the Li-COR Odyssey CLx. Quantification was performed using Image Studio Software (Li-COR). Blots were stripped using NewBlot PVDF Stripping Buffer (Li-COR) according to the manufacturer's protocol.

3.5.2 Protein Expression and Purification

For each protein construct, five 15-cm plates of 90% confluent HEK-293T cells in 20 mL complete DMEM were transfected with 20-30 μg plasmid using poly(ethyleneimine) (23966-2, Polysciences, Inc.). Briefly, DNA was diluted in 2 mL pre-warmed, serum-free DMEM and PEI (1 mg/mL in sterile ddH_2O) was added dropwise with vigorous shaking at a 3:1 w/w PEI/DNA ratio. DNA/PEI complexes were allowed to form for 20 min at RT and then added dropwise to each plate. After 24 h, the medium in each plate was replaced with DMEM containing 2% FBS and 1x P/S. Sometimes, proteins were found to be truncated

once secreted into the medium. To prevent this, the medium was supplemented with 0.5x cOmplete protease inhibitor cocktail without ETDA (PIC-, 11697498001, Sigma Aldrich). At 3 d post-transfection, the medium was harvested and centrifuged to remove cell debris. A new 20-mL aliquot of DMEM, 2% FBS, 1x P/S was added, which was harvested 2 d later, centrifuged, and combined with the first aliquot. The solution pH was adjusted to 8.0 using 2 M Tris, and medium was rotated end-over-end for 2 h at 4 °C with 500 μL Ni-NTA resin (Qiagen) prewashed twice with PBS. The resin was separated from the medium by centrifugation and loaded onto a disposable column (Bio-Rad). The resin was washed with 10 mL phosphate wash buffer (100 mM sodium phosphate pH 7.4, 300 mM NaCl, 10 mM imidazole), and protein was eluted with two aliquots of 1 mL elution buffer (50 mM sodium phosphate pH 7.4, 150 mM NaCl, 250 mM imidazole). Elution samples were combined and buffer exchanged by centrifugation with PBS. Samples were stored at 4 °C for up to one week or flash-frozen and stored at -20 °C.

3.5.3 Protein-GAG Binding Assays.

Carbohydrate enzyme-linked immunosorbent assay. Biotinylated CS-E and HS were prepared as previously described.[38] Initial ELISAs were performed with commercially available Tie1- and Tie2-Fc conjugates (R&D Systems). Wells of Protein A/G 8-well strips (ThermoFisher Scientific) were rinsed twice with 200 μL PBST (PBS + 0.02% Tween-20) and then incubated with 100 μL 10 μg/mL Tie1-Fc or Tie2-Fc in 1% bovine serum albumin (BSA, Fisher Scientific) in PBS for

1 h at RT with gentle rocking. Wells were rinsed thrice with PBST and next incubated with 200 μL 5% BSA in PBS for 1 h at RT. During this incubation step, a dilution series of biotinylated CS-E or HS was produced in PBS. Wells were again rinsed thrice with PBST, and 50 μL of each GAG-containing solution was added to the wells. Wells were incubated with GAG-containing solutions for 3 h at RT with gentle rocking. Wells were rinsed four times with PBST and then incubated with 100 μL 1:15000 HRP-conjugated streptavidin (ThermoFisher Scientific) for 1 h at RT with gentle rocking. Wells were again rinsed four times with PBST and then incubated with 100 μL development solution (R&D Systems) for 15 min at RT in the dark. Reactions were quenched by the addition of 100 μL 2 N H_2SO_4, and absorbance was read at 450 nm. Assays were performed in duplicate for each concentration, and values were reported as the average ± SEM. Curves were fitted and K_D values were calculated with Prism 7 (GraphPad) using the nonlinear curve fitting of standard binding with Hill slope function. For experiments using over-expressed, purified proteins, protein concentrations were first normalized using the bicinchoninic acid (BCA) assay (ThermoFisher Scientific) and used the same as the purchased proteins mentioned above.

GAG microarrays. GAG microarrays were generated and conducted as previously described.[33] Briefly, slides were blocked with 10% FBS in PBS for 1 h at RT. Stock solutions of Tie1-Fc, Tie2-Fc, Ang1, and Ang4 (2 μM) were prepared in sterile PBS containing 1% BSA. Blocked slides were washed once with PBS and slowly rocked with 150 μL of 1% BSA/PBS containing 1 μM Tie1-Fc for 2 h at RT. For

ternary complex formation, 150 μL of 1% BSA/PBS containing 1 μM Tie2-Fc with or without 1 μM ligand (*i.e.*, 1 μM Tie2-Fc ± 1 μM Ang1; 1 μM Tie2-Fc ± 1 μM Ang4) were used immediately without prior incubation. Slides were washed three times with PBS and incubated with an AF647-conjugated goat anti-human Fc antibody (1:5000) in 1% BSA/PBS for 1 h at RT in the dark with gentle rocking. Slides were then washed three times with PBS and twice with ddH_2O and blown dry under a stream of filtered air. Arrays were scanned using a G2565BA DNA Microarray Scanner (Agilent), and fluorescence was quantified using GenePix 5.0 software (Molecular Devices) with normalization against local background. The data represent the average of 10 spots per concentration of polysaccharide.

Surface plasmon resonance. All experiments were conducted using a Biacore T200 instrument (GE Healthcare). A CM5 sensor chip (GE Healthcare) was first functionalized with streptavidin using the manufacturer's amine coupling protocol. Briefly, all flow cells of a CM5 sensor chip (GE Healthcare) were incubated with a 1:1 molar ratio of *N*-hydroxysuccinimide and 1-ethyl-3-(3-dimethylaminopropyl)carbodiimide for 3 min at a flow rate of 10 μL/min followed by 1 μM streptavidin in 0.01 NaOAc pH 5.0 until the response rate leveled off (saturating the flow cell surface). Remaining reactive groups were quenched by ethanolamine. Solutions of biotinylated CS-E or HS were then each flowed over one of the four flow cells (CS-E: flow cell 2; HS: flow cell 4) to provide a response value of roughly 25 RU. As a control, an antibody specific to CS-E was flowed over the CS-E containing flow cell and corresponding control

cell to ensure successful loading of biotinylated GAG. To test binding of Tie1-Fc to the biotinylated GAGs, a two-fold dilution series of Tie1-Fc (starting at 100 nM) was produced and flowed over the flow cells for 300 s at a rate of 20 μL/min. Dissociation of Tie1-Fc was then monitored for 350 s using the same flow rate. Between each run, the surface was regenerated using 2.5 M $MgCl_2$ at a flow rate of 30 μL/min. Response values are reported after substraction of the control (-GAG) cell. The resulting curves were fit to the one-to-one Langmuir binding model equation using the Biacore SPR evaluation software.

3.5.4 Computational Methods

Structure modeling. The Tie1 homology model was constructed using the program SWISS-MODEL[42] with human Tie2 ligand-binding domain (PDB ID 2GY5)[41] as a template and the sequence of human Tie1 (UniProt ID P35590). The Tie1 homology model was briefly minimized in vacuum using the DREIDING force field[70] to reduce steric clashes built into the model. To produce the GAG ligand for docking, a dodecasaccharide structure was first generated for CS-E and HS, and the ligand side chains were relaxed by a brief minimization step. Ligands were then placed in a water box, and a molecular dynamics (MD) simulation was run for 5 ns. The structure closest to the average structure over the 5 ns MD run was selected as the conformation for docking. The dodecasaccharide was then truncated to a hexasaccharide by removing three monosaccharides from the reducing and non-reducing ends.

Docking and binding site determination. First, a coarse round of docking is performed. Here the ligand is docked to the entire protein surface. Prior to the docking run, the protein structure is "alanized" by replacing bulky, nonpolar residues (Val, Leu, Ile, Met, Phe, Try, and Trp) with Ala to allow for more complete sampling of the binding site. The protein is split into regions, and spheres are generated for docking. For each region, docked ligand poses are generated, scored, and clustered into families based on energy and root-mean-square deviation. For each cluster, the lowest energy pose known as the family head is output, generally producing 120 poses for each docked region. These poses are then de-alanized and undergo side chain optimization using SCREAM[71] to produce a unique set of protein side chain conformations for each pose. The top docking regions are identified by ranking the average energy of the top five poses in each region. Top regions are then subjected to an additional round of docking. Here a minimization step is performed to improve protein-ligand interactions following side chain placement and optimization with SCREAM. These poses are clustered as before, and family heads are output. The scoring energy known as the snap binding energy used to rank poses is equal to the complex energy minus protein energy and ligand energy.

3.5.5 Biological Assays

Cell-surface crosslinking. EA.hy926 cells were plated onto precoated six-well plates and grown to confluency with complete DMEM. Cells were rinsed three times with ice-cold PBS and then incubated with 100 μL 1 mM DTSSP in PBS (freshly

prepared) for 30 min at RT with gentle rocking. Unreacted DTSSP was quenched by addition of 5 μL 1 M Tris pH 8.0 with incubation for 15 min at RT. The crosslinking solution was then removed, and cells were lysed by scraping with ice-cold 200 μL Triton lysis buffer (20 mM HEPES pH 7.9, 150 mM NaCl, 1% Triton X-100, 5% glycerol, 1x PIC-). Lysates were rotated end-over-end for 10 min at 4 °C and then centrifuged for 10 min at 21,000 x *g* to remove all insoluble material. The lysates were transferred to new tubes and rotated end-over-end with 1 μg Gt anti-Tie1 (AF619, R&D Systems) overnight at 4 °C. The next day, 20 μL magnetic Protein A/G beads (ThermoFisher Scientific) prewashed with HBS (50 mM HEPES pH 7.9, 150 mM NaCl) was added to each sample and rotated end-over-end for 1 h at 4 °C. Beads were then washed with 500 μL HBS, 0.1% Triton X-100 thrice for 5 min at 4 °C. After the final wash, all wash buffer was removed, and the beads were resuspended in 30 μL 1x SDS-PAGE loading buffer + 20 mM DTT (freshly prepared) and heated to 95 °C for 10 min. Samples were processed for Western blotted as described above. Blots were probed with 1 μg/mL Gt anti-Tie1 (AF619, R&D Systems), 1 μg/mL Gt anti-Tie2 (AF313, R&D Systems), and 1 μg/mL Gt anti-α_5 integrin (AF1864, R&D Systems).

Proximity ligation assays. EA.hy926 cells were plated onto precoated 96-well glass bottom plates and grown to confluency. Cells were then washed twice with PBS and then fixed with 4% paraformaldehyde in PBS for 20 min at RT. Cells were rinsed thrice with PBS and blocked with the DuoLink blocking buffer (Sigma Aldrich) for 1 h at RT. Cells were rinsed twice with PBS and incubated overnight

at 4 °C with 1:100 Ms anti-Tie1 (MAB619, R&D Systems) and 1:100 Rb anti-Tie2 (H176, Santa Cruz Biotechnology) in 1% BSA/PBS. Cells were then carried through the Duolink labeling protocol scaled to 30 μL reactions per well according to the manufacturer's protocol (DUO92101, Sigma Aldrich). Cells were visualized using an LSM 710 confocal microscope (Zeiss) with a 40x oil immersion objective and preset filter settings for Texas Red and DAPI. A *Z*-stack of images was collected for each field of view, and a single image was produced using maximal pixel intensity.

Lentivirus production. Lentiviruses were produced by co-transfecting two to four 10-cm plates of 90% confluent HEK-293T cells in complete DMEM with the HTP lentiviral plasmid and pLP1, pLP2, and VSV-G helper plasmids (ThermoFisher Scientific) at 4.3 μg, 6.2 μg, 3.1 μg, and 3.7 μg, respectively, using Lipofectamine 3000 (ThermoFisher Scientific) according to the manufacturer's protocol. Medium was harvested and replaced with complete DMEM at 24, 48, and 72 h, centrifuged to remove cell debris, and combined. Lentivirus particles were either directly flash frozen and stored at -80 °C or were concentrated by PEG-6000 precipitation as previously described.[69] Precipitated lentiviruses were resuspended in complete DMEM, flash frozen, and stored at -80 °C.

Generation and validation of EA.hy926-HTP cell line. EA.hy926 cells were grown to 80% confluency in a six-well plate with complete DMEM and then treated with 0-20 μL of the concentrated HTP-LV stock along with 8 μg/mL polybrene (Sigma Aldrich). After 48 h, cells were split 1:3 into new six-well plates in complete

DMEM containing 5 μg/mL blasticidin (InvivoGen). Medium was changed every 2 d. After roughly 1-1.5 weeks, all cells in the untreated well had died. Cells were treated for an additional 3 d with 5 μg/mL blasticidin, and cells from the well treated with the lowest amount of lentivirus that survived selection were expanded and cryo-preserved. To validate expression of HTP, treated and untreated EA.hy926 cells were plated onto precoated 96-well glass bottom plates and allowed to grow to confluency. Cells were then treated with 1:1000 cell impermeable AlexaFluor 488-conjugated HTL (G1001, Promega) and 1:1000 Hoescht 33342 (H3750, ThermoFisher Scientific) in complete DMEM at 37 °C for 15 min. Cells were rinsed thrice with complete DMEM and live imaged on an LSM 710 confocal microscope (Zeiss) with a 10x objective.

Glycan engineering and stimulation assay. EA.hy926-HTP cells were treated in suspension with 2 U/mL heparinase I/III in complete DMEM for 2 h at 37 °C with gentle mixing every 15 min. Cells were then plated on precoated six-well plates at 100,000 cells per well and grown overnight at 37 °C with complete DMEM. The following day, medium was replaced with serum-starved DMEM (0.5% FBS) containing 5 μg/mL de-HS-CL or HS-CL for 2 h. Medium was removed, and cells were treated with serum-starved DMEM for an additional 4 h. Cells were then stimulated with serum-starved DMEM containing 500 ng/mL Ang1, Ang2, or Ang4 or no ligand for 30 min at 37 °C. Cells were rinsed with ice-cold PBS and then lysed in 200 μL SDS lysis buffer (50 mM Tris pH 7.6, 150 mM NaCl, 1% SDS, 1x PIC-, 1x Phos-STOP (Sigma Aldrich)) at RT. Lysates were sonicated for 10 s at

40% intensity to sheer DNA and then centrifuged for 5 min at 21,000 x *g* to remove any insoluble debris. Lysates were subjected to Western blotting as described above. Blots were probed using 1:1000 Rb anti-phosphoAkt(T308) and 1:1000 Ms anti-Akt (9275 and 9272, Cell Signaling Technology). Assay was performed in triplicate. Phospho-Akt values were normalized to total Akt levels and are reported as the average value as normalized to the untreated de-HS-CL control. Statistical analysis was performed by Prism 7 (GraphPad) using a two-way ANOVA with Sidak's multiple comparisons test.

3.5.6 Transgenic Tie1 Mouse Model

Generating and testing gRNA sequences. Murine Tie1 gDNA was amplified from a C57BL/6J mouse gDNA sample (Jackson Laboratories) purified by DNEasy Blood and Tissue Kit (Qiagen) using the Q5 2x hot-start PCR master mix (New England Biolabs) using the following primers:

```
Tie1-EGxxFP-F:
CGTGCTGCTGCCCGACAACCACTGAGGATCCGTGCTGTGGATGAGAGGTAAGTT
Tie1-EGxxFP-R:
GGGTCAGCTTGCCGATATCGAATTCGTCGACGAAGAGGCTTGCAGGTAAAGAGC
```

The amplified region was gel purified and cloned into the pCAG-EGxxFP vector between BamHI and SalI sites. Correct incorporation of the sequence was validated using Sanger sequencing with the following primer:

```
EGxxFP-Seq: CTACAACAGCCACAACGTCTAT
```

Guide RNA sequences were designed using the online CHOPCHOP tool (http://chopchop.cbu.uib.no/) against the Dec. 2011 (GRCm38/mm10) murine

genome assembly against regions surrounding the Tie1 Arg-38 and Arg-82 codons. Sequences were selected based on predicted activity and minimal off-target homology. Primers to clone these gRNA sequences into the pX459 vector are shown below:

Tie1 Arg-82:

Tie1-gRNA-1F: CACCGGTGAGAACCGTTGCGTGCC
Tie1-gRNA-1R: TTTGGGCACGCAACGGTTCTCACC
Tie1-gRNA-2F: CACCGTTCTCACCAGGTCACGCTG
Tie1-gRNA-2R: TTTGCAGCGTGACCTGGTGAGAAC
Tie1-gRNA-3F: CACCGGCACGCAACGGTTCTCACC
Tie1-gRNA-3R: TTTGGGTGAGAACCGTTGCGTGCC
Tie1-gRNA-4F: CACC**G**ATCGTGCGCACCTTCCCGCC
Tie1-gRNA-4R: TTTGGGCGGGAAGGTGCGCACGAT**C**

Tie1 Arg-38:

Tie1-gRNA-5F: CACC**G**CGCAGGTCAGGAAGAAACGC
Tie1-gRNA-5R: AAACGCGTTTCTTCCTGACCTGCG**C**
Tie1-gRNA-6F: CACCGTCCGAGCTCCTCCCTGCTC
Tie1-gRNA-6R: AAACGAGCAGGGAGGAGCTCGGAC
Tie1-gRNA-7F: CACC**G**TTCTTCCTGACCTGCGTGTC
Tie1-gRNA-7R: AAACGACACGCAGGTCAGGAAGAA**C**
Tie1-gRNA-8F: CACC**G**CCTGACCTGCGTGTCTGGTG
Tie1-gRNA-8R: AAACCACCAGACACGCAGGTCAGG**C**
Tie1-gRNA-9F: CACC**G**CCTCACCAGACACGCAGGTC
Tie1-gRNA-9R: AAACGACCTGCGTGTCTGGTGAGG**C**

For gRNA sequences that did not begin with G, a single G:C bp was added (shown in bold) to the primers to allow for efficient transcription by RNA polymerase III. gRNA oligonucleotides were dissolved at 100 μM in ddH_2O, and annealing/phosphorylation reactions were set up as follows: 1 μL forward primer, 1 μL reverse primer, 1 μL 10x T4 ligation buffer, 6.5 μL ddH_2O, 0.5 μL T4 PNK. Reactions were incubated using a thermocycler at 37 °C for 30 min, followed by

95 °C for 5 min and ramping down to 25 °C at 5 °C/min. The reaction mixture was diluted 1:250 in ddH_2O and used in digestion/ligation reactions as follows: 100 ng pX459 vector, up to 12.5 μL with ddH_2O, 2 μL 1:250 diluted reaction, 1 μL 10 mM DTT, 1 μL 10 mM ATP, 2 μL 10x FastDigest buffer (ThermoFisher Scientific), 1 μL FastDigest BpiI, 0.5 μL T7 DNA ligase. Reactions were incubated for six cycles of 5 min at 37 °C then 5 min at 23 °C and could then be used for transformation. Correct incorporation of the gRNA sequence was validated with Sanger sequencing using the following primer:

U6-F-Seq: GACTATCATATGCTTACCGT

To test gRNAs, confluent six-well plates of HEK-293T cells were transfected with 0.5 μg pCAG-EG(Tie1)FP with 0.5 μg of each of the gRNA-containing pX459 vectors. After 48 h, cells were live imaged using an LSM 710 confocal microscope (Zeiss) with a 5x objective using GFP filter sets. gRNA efficiency was estimated by the percentage of GFP^+ cells. gRNA1 and gRNA5 were the best performing gRNA sequences for Arg-82 and Arg-38 regions, respectively.

Designing repair template. The repair template to be used for injection was designed either as a pair of single stranded oligonucleotides (ssODNs) or a larger double stranded DNA (dsDNA) fragment. In both cases, mutations for Arg-to-Ala and silent mutations disrupting the NGG PAM sequence were added. The R38A mutation produced a StuI restriction site, and a silent mutation was introduced at R82A to produce an EaeI restriction site to be used for rapid genotyping. ssODNs and dsDNA were purchased as DNA Ultramers and a gBlock gene fragment,

respectively (Integrated DNA Technologies). The sequences for the repair templates are shown below, with mutations bolded, the Arg-82 codon in green, and the Arg-38 codon in orange.

ssODN (Arg-38):

caggggcgggtccgagctcctccctgctccggcctcaccagacacgcaggtcaggaa
gaaGGCctg**A**gggtctgtgatgcgcaggttggccagcaatgttaagtcaacagacgc
acctaggaccaaa

ssODN (Arg-82):

gacgcctaccaaatccgagggcttggagaagcccctcagcgtgacctggtgagaacc
gtt**GGCG**gccag**A**tacaggggctgcccaggcgggaaggtgcgcacgatgcgatcatc
cttctccagcagcagg

dsDNA:

cgcaggctcctggtccttttagtacagtaggagggtggctcagagctacagatgaga
gggaagcccctagaggttggtcacaaggatggcaggtgggtcagggtggactaagta
tatggtgggccatggatggaagacctaaggtgtcagcatcatgggtctccctgtccc
accaactgcccctcaccgttgttcttccagatcacgtcagtctgcttttccttgtgc
acatgggcagaaagcacagcagtgtcacctttgttcaccgtgtgtgtgaccttgtct
ggaaacaggtgtgctgtggatgagaggtaagttcagcgatctacaacacagccctcc
ctctggtggtcgatctcctggtaggccagactcacccctgggctgttgtgcacata
gagaactcgagtgcgccgcgcgccagcaccacccacacaggagaagacgcctaccaa
atccgagggcttggagaagcccctcagcgtgacctggtgagaaccgtt**GGCG**gccag
Atacaggggctgcccaggcgggaaggtgcgcacgatgcgatcatccttctccagcag
caggggcgggtccgagctcctccctgctccggcctcaccagacacgcaggtcaggaa
gaaGGCctg**A**gggtctgtgatgcgcaggttggccagcaatgttaagtcaacagacgc
acctaggaccaaacaacagtgactccatggtggatcctgccagctcagcagccccag
gagcccgggactccaacagtaacttgtgttaatatttcactgtgtccttagaagact
tcacttttcaaagatttccgcccattcccttcccttacacatgtgctcgctcttta
cctgcaagcctcttcgtcctaaaacataaacaaaagcacacatccttctctggtcca
gacagggaatgagctacgcttctgtctccttcccttactctgtccgtgtcaggtcat
tgccctgactcctgtgtgaaccattcccaccaaggctatccctgagccacctgtccc
tgccccatcatggaggtgcaggttagaagagtcgctgagactggagtgtcatgagga
cgcacaccctctttcttgcttaactaattgaggactatttgactggctgggattgaa
gatcggttagggccagagagacacagacacaggtgggtctgggccctaccttgggaa
gctggaggaccagacacaggcatccctcccagatggaggtgttggctcagagggagg
aacatctaaccagcaggggggcgggggaaggaaaggggacaggaaaagatgcagata
acaaacttcattagaaggtgcttgggtgaggaggaacgaaaggtcaggcgtagggag
aggccaccctacgctcaagtatgagaaatgttgtagtgtggggaggggagctgcccc

gggctagtgcaactggagcgtaaaatctgtaccctgaagtgggcaagaccgaggaga
agaatgtgatcagcctgct

Preparation of injection mixture. gRNAs were purchased as the crRNA/tracrRNA system from Integrated DNA Technologies. These constructs contain chemical modifications to increase RNA stability. RNA molecules were dissolved in sterile injection buffer (1 mM Tris pH 7.5, 0.1 mM EDTA) at 1 μg/μL. Mature crRNA:tracrRNA complexes were produced by combining 5 μL 1 μg/μL crRNA and 10 μL 1 μg/μL tracrRNA. Samples were incubated in a thermocycler at 95 °C for 5 min and then ramped down to 25 °C at 5 °C/min. Samples were diluted two-fold in injection buffer, and 4 μL of each complex was combined along with 64 μL injection buffer. Cas9 protein (Integrated DNA Technologies) was diluted to 500 ng/μL in injection buffer, and 8 μL was added to the RNA mixture. Samples were incubated at RT for 15 min. The Cas9/gRNA mixture was aliquoted at 20 μL, and either 1 μL 500 ng/μL ssODN (Arg-82 and Arg-38) or 2.5 or 5 μL 100 ng/μL dsDNA repair template was added with injection buffer to achieve 25 μL total. Samples were centrifuged for 10 min at 21,000 x *g*, and 20 μL was transferred to a new tube. The final concentrations of the injection solution were 20 ng/μL each gRNA/Cas9 complex and 10 or 20 ng/μL repair template. Roughly 20 zygotes per condition from superovulated, mated B6SJL-F1/J (Jackson Laboratories) were harvested and cultured. The injection mixture was pronuclear injected into each zygote, and zygotes were allowed to develop for 3 d.

Blastocyst genotyping. Blastocysts were aliquoted into a V-bottom 96-well plate in 10 μL culture medium and flash frozen. To each well, 10 μL 2x blastocyst lysis buffer (200 mM Tris pH 8.3, 200 mM KCl, 0.02% gelatin, 0.45% Tween-20, 60 μg/mL yeast tRNA, 125 μg/mL proteinase K) was added and allowed to incubate for 5 min. Samples were mixed by pipetting, transferred to PCR tubes, and incubated for 10 min at 56 °C and 10 min at 95 °C. gDNA was amplified in two rounds of nested PCR with Q5 2x Hot-Start Master Mix (New England Biolabs). First, a 25 μL reaction was set up using 4 μL lysate and amplified for 35 cycles with annealing temperature of 65 °C. Next, 4 μL of the first reaction was using for a second PCR reaction using a second set of primers with the same annealing temperature. Primers used are shown below:

```
Tie1-gDNA-Geno-F1: AGAGCTACAGATGAGAGGGAAG
Tie1-gDNA-Geno-F2: CTAGAGGTTGGTCACAAGGATG
Tie1-gDNA-Geno-R1: CACATTCTTCTCCTCGGTCTTG
Tie1-gDNA-Geno-R2: TCACCCAAGCACCTTCTAATG
```

Amplicons were gel purified and submitted for Sanger sequencing using the second forward primer.

For production of litters, roughly 80 zygotes were injected once per day for four days. Once zygotes had proceeded to the blastocyst stage, they were implanted into surrogate B6SJL-F1/J mice. Successful litters were tailed for genotyping. gDNA from tail samples was harvested using the DNEasy Kit and amplified in a single step using F1/R1 genotyping primers listed above. Amplicons were gel purified and submitted for Sanger sequencing using the F2 primer.

3.6 References

1. J. Partanen *et al.* A novel endothelial cell surface receptor tyrosine kinase with extracellular epidermal growth factor homology domains. *Mol Cell Biol.* **1992**, *12*: 1698-1707.
2. D. J. Dumont, T. P. Yamaguchi, R. A. Conlon, J. Rossant, M. L. Breitman. Tek, a novel tyrosine kinase gene located on mouse chromosome 4, is expressed in endothelial cells and their presumptive precursors. *Oncogene.* **1992**, *7*: 1471-1480.
3. T. N. Sato, Y. Qin, C. A. Kozak, K. L. Audus. Tie-1 and Tie-2 define another class of putative receptor tyrosine kinase genes expressed in early embryonic vascular system. *Proc Natl Acad Sci USA*. **1993**, *90*: 9355-9358.
4. A. Iwama *et al.* Molecular cloning and characterization of mouse TIE and TEK receptor tyrosine kinase genes and their expression in hematopoietic stem cells. *Biochem Biophys Res Commun.* **1993**, *195*: 301-309.
5. S. Davis *et al.* Isolation of angiopoietin-1, a ligand for the TIE2 receptor, by secretion-trap expression cloning. *Cell.* **1996**, *87*: 1161-1169.
6. P. C. Maisonpierre *et al.* Angiopoietin-2, a natural antagonist for Tie2 that disrupts in vivo angiogenesis. *Science.* **1997**, *277*: 55-60.
7. D. M. Valenzuela *et al.* Angiopoietins 3 and 4: diverging gene counterparts in mice and humans. *Proc Natl Acad Sci USA*. **1999**, *96*: 1904-1909.
8. N. Jones, K. Iljin, D. J. Dumont, K. Alitalo. Tie receptors: new modulators of angiogenic and lymphangiogenic responses. *Nat Rev Mol Cell Biol.* **2001**, *2*: 257-267.

9. H. G. Augustin, G. Y. Koh, G. Thurston, K. Alitalo. Control of vascular morphogenesis and homeostasis through the angiopoietin-Tie system. *Nat Rev Mol Cell Biol.* **2009**, *10*: 165-177.

10. P. Saharinen, M. Jeltsch, M. M. Santoyo, V.-M. Leppänen, K. Alitalo. *The TIE receptor family*. In: D. L. Wheeler, Y. Yarden, Eds., *Receptor Tyrosine Kinases: Family and Subfamilies*. Ed.: Humana Press; 2015.

11. D. J. Dumont *et al.* Dominant-negative and targeted null mutations in the endothelial receptor tyrosine kinase, tek, reveal a critical role in vasculogenesis of the embryo. *Genes Dev.* **1994**, *8*: 1897-1909.

12. T. N. Sato *et al.* Distinct roles of the receptor tyrosine kinases Tie-1 and Tie-2 in blood vessel formation. *Nature.* **1995**, *376*: 70-74.

13. M. C. Puri, J. Rossant, K. Alitalo, A. Bernstein, J. Partanen. The receptor tyrosine kinase TIE is required for integrity and survival of vascular endothelial cells. *EMBO J.* **1995**, *14*: 5884-5891.

14. G. D'Amico *et al.* Loss of endothelial Tie1 receptor impairs lymphatic vessel development-brief report. *Arterioscler Thromb Vasc Biol.* **2010**, *30*: 207-209.

15. X. Qu, K. Tompkins, L. E. Batts, M. Puri, H. S. Baldwin. Abnormal embryonic lymphatic vessel development in Tie1 hypomorphic mice. *Development.* **2010**, *137*: 1285-1295.

16. X. Qu, B. Zhou, H. S. Baldwin. Tie1 is required for lymphatic valve and collecting vessel development. *Dev Biol.* **2015**, *399*: 117-128.

17. K. V. Woo *et al.* Tie1 attenuation reduces murine atherosclerosis in a dose-dependent and shear stress-specific manner. *J Clin Invest.* **2011**, *121*: 1624-1635.

18. G. D'Amico *et al.* Tie1 deletion inhibits tumor growth and improves angiopoietin antagonist therapy. *J Clin Invest.* **2014**, *124*: 824-834.

19. H. Huang, A. Bhat, G. Woodnutt, R. Lappe. Targeting the ANGPT-TIE2 pathway in malignancy. *Nat Rev Cancer*. **2010**, *10*: 575-585.

20. S. Han *et al.* Amelioration of sepsis by TIE2 activation-induced vascular protection. *Sci Transl Med*. **2016**, *8*: 335ra355.

21. H. J. Lee *et al.* Biological characterization of angiopoietin-3 and angiopoietin-4. *FASEB J*. **2004**, *18*: 1200-1208.

22. S. Savant *et al.* The Orphan Receptor Tie1 Controls Angiogenesis and Vascular Remodeling by Differentially Regulating Tie2 in Tip and Stalk Cells. *Cell Rep*. **2015**, *12*: 1761-1773.

23. S. B. Mueller, C. D. Kontos. Tie1: an orphan receptor provides context for angiopoietin-2/Tie2 signaling. *J Clin Invest*. **2016**, *126*: 3188-3191.

24. H. Singh, T. A. Tahir, D. O. Alawo, E. Issa, N. P. Brindle. Molecular control of angiopoietin signalling. *Biochem Soc Trans*. **2011**, *39*: 1592-1596.

25. T. C. Seegar *et al.* Tie1-Tie2 interactions mediate functional differences between angiopoietin ligands. *Mol Cell*. **2010**, *37*: 643-655.

26. E. A. Korhonen *et al.* Tie1 controls angiopoietin function in vascular remodeling and inflammation. *J Clin Invest*. **2016**, *126*: 3495-3510.

27. J. Schlessinger *et al.* Crystal structure of a ternary FGF-FGFR-heparin complex reveals a dual role for heparin in FGFR binding and dimerization. *Mol Cell*. **2000**, *6*: 743-750.

28. C. Rolny, D. Spillmann, U. Lindahl, L. Claesson-Welsh. Heparin amplifies platelet-derived growth factor (PDGF)-BB-induced PDGF alpha -receptor but not PDGF beta -receptor tyrosine phosphorylation in heparan sulfate-deficient cells. Effects on signal transduction and biological responses. *J Biol Chem*. **2002**, *277*: 19315-19321.

29. D. Xu, M. M. Fuster, R. Lawrence, J. D. Esko. Heparan sulfate regulates $VEGF_{165}$- and $VEGF_{121}$-mediated vascular hyperpermeability. *J Biol Chem.* **2011**, *286*: 737-745.

30. L. E. Kemp, B. Mulloy, E. Gherardi. Signalling by HGF/SF and Met: the role of heparan sulphate co-receptors. *Biochem Soc Trans.* **2006**, *34*: 414-417.

31. V. Koprivica *et al.* EGFR activation mediates inhibition of axon regeneration by myelin and chondroitin sulfate proteoglycans. *Science.* **2005**, *310*: 106-110.

32. M. W. Barnett, C. E. Fisher, G. Perona-Wright, J. A. Davies. Signalling by glial cell line-derived neurotrophic factor (GDNF) requires heparan sulphate glycosaminoglycan. *J Cell Sci.* **2002**, *115*: 4495-4503.

33. C. J. Rogers *et al.* Elucidating glycosaminoglycan-protein-protein interactions using carbohydrate microarray and computational approaches. *Proc Natl Acad Sci USA*. **2011**, *108*: 9747-9752.

34. P. B. Murray. Heparin is an activating ligand of the orphan receptor tyrosine kinase ALK. *Sci Signal*. **2015**, *8*: ra6.

35. G. Bezakova, M. A. Ruegg. New insights into the roles of agrin. *Nat Rev Mol Cell Biol.* **2003**, *4*: 295-308.

36. T. Arai, A. Parker, W. Busby, Jr., D. R. Clemmons. Heparin, heparan sulfate, and dermatan sulfate regulate formation of the insulin-like growth factor-I and insulin-like growth factor-binding protein complexes. *J Biol Chem.* **1994**, *269*: 20388-20393.

37. M. Teran, M. A. Nugent. Synergistic binding of vascular endothelial growth factor-A and its receptors to heparin selectively modulates complex affinity. *J Biol Chem.* **2015**, *290*: 16451-16462.

38. J. M. Brown *et al.* A sulfated carbohydrate epitope inhibits axon regeneration after injury. *Proc Natl Acad Sci USA*. **2012**, *109*: 4768-4773, S4768/4761-S4768/4710.

39. C. J. Rogers *et al.* Chondroitin sulfate E influences retinotopic mapping via EphB3. *in preparation*. **2017**.

40. G. J. Miller *et al.* Chondroitin sulfate E mediates axonal inhibition via EphA4 activation. *in preparation*. **2017**.

41. W. A. Barton *et al.* Crystal structures of the Tie2 receptor ectodomain and the angiopoietin-2-Tie2 complex. *Nat Struct Mol Biol.* **2006**, *13*: 524-532.

42. L. Bordoli *et al.* Protein structure homology modeling using SWISS-MODEL workspace. *Nat Protoc*. **2009**, *4*: 1-13.

43. K. Iljin *et al.* A fluorescent Tie1 reporter allows monitoring of vascular development and endothelial cell isolation from transgenic mouse embryos. *FASEB J.* **2002**, *16*: 1764-1774.

44. G. Li *et al.* Glycosaminoglycanomics of cultured cells using a rapid and sensitive LC-MS/MS approach. *ACS Chem Biol.* **2015**, *10*: 1303-1310.

45. S. R. Hubbard, W. T. Miller. Receptor tyrosine kinases: mechanisms of activation and signaling. *Curr Opin Cell Biol.* **2007**, *19*: 117-123.

46. P. Saharinen *et al.* Multiple angiopoietin recombinant proteins activate the Tie1 receptor tyrosine kinase and promote its interaction with Tie2. *J Cell Biol.* **2005**, *169*: 239-243.

47. H. T. Yuan *et al.* Activation of the orphan endothelial receptor Tie1 modifies Tie2-mediated intracellular signaling and cell survival. *FASEB J.* **2007**, *21*: 3171-3183.

48. M. B. Marron, D. P. Hughes, M. D. Edge, C. L. Forder, N. P. Brindle. Evidence for heterotypic interaction between the receptor tyrosine kinases TIE-1 and TIE-2. *J Biol Chem.* **2000**, *275*: 39741-39746.

49. C. D. Kontos, E. H. Cha, J. D. York, K. G. Peters. The endothelial receptor tyrosine kinase Tie1 activates phosphatidylinositol 3-kinase and Akt to inhibit apoptosis. *Mol Cell Biol.* **2002**, *22*: 1704-1713.

50. V. M. Leppanen, P. Saharinen, K. Alitalo. Structural basis of Tie2 activation and Tie2/Tie1 heterodimerization. *Proc Natl Acad Sci USA*. **2017**, *114*: 4376-4381.

51. A. C. Dalton, T. Shlamkovitch, N. Papo, W. A. Barton. Constitutive Association of Tie1 and Tie2 with Endothelial Integrins is Functionally Modulated by Angiopoietin-1 and Fibronectin. *PLoS One.* **2016**, *11*: e0163732.

52. O. Söderberg *et al.* Direct observation of individual endogenous protein complexes in situ by proximity ligation. *Nat Methods.* **2006**, *3*: 995-1000.

53. N. Oh *et al.* A designed angiopoietin-1 variant, dimeric CMP-Ang1 activates Tie2 and stimulates angiogenesis and vascular stabilization in *N*-glycan dependent manner. *Sci Rep.* **2015**, *5*: 15291.

54. E. Forsberg, L. Kjellen. Heparan sulfate: lessons from knockout mice. *J Clin Invest*. **2001**, *108*: 175-180.

55. J. R. Bishop, M. Schuksz, J. D. Esko. Heparan sulphate proteoglycans fine-tune mammalian physiology. *Nature.* **2007**, *446*: 1030-1037.

56. P. D. Hsu, E. S. Lander, F. Zhang. Development and applications of CRISPR-Cas9 for genome engineering. *Cell.* **2014**, *157*: 1262-1278.

57. H. Wang, M. La Russa, L. S. Qi. CRISPR/Cas9 in Genome Editing and Beyond. *Annu Rev Biochem.* **2016**, *85*: 227-264.

58. A. C. Komor, A. H. Badran, D. R. Liu. CRISPR-Based Technologies for the Manipulation of Eukaryotic Genomes. *Cell.* **2017**, *168*: 20-36.

59. H. Yang *et al.* One-step generation of mice carrying reporter and conditional alleles by CRISPR/Cas-mediated genome engineering. *Cell.* **2013**, *154*: 1370-1379.

60. C. Tong, G. Huang, C. Ashton, P. Li, Q. L. Ying. Generating gene knockout rats by homologous recombination in embryonic stem cells. *Nat Protoc.* **2011**, *6*: 827-844.

61. D. Paquet *et al.* Efficient introduction of specific homozygous and heterozygous mutations using CRISPR/Cas9. *Nature.* **2016**, *533*: 125-129.

62. D. Mashiko *et al.* Generation of mutant mice by pronuclear injection of circular plasmid expressing Cas9 and single guided RNA. *Sci Rep.* **2013**, *3*: 3355.

63. M. Srivastava *et al.*, An inhibitor of nonhomologous end-joining abrogates double-strand break repair and impedes cancer progression. *Cell (Cambridge, Massachusetts).* **2012**, *151*: 1474-1487.

64. Y. Xu, Q. Yu, Angiopoietin-1, Unlike Angiopoietin-2, Is Incorporated into the Extracellular Matrix via Its Linker Peptide Region. *J Biol Chem.* **2001**, *276*: 34990-34998.

65. Y. Xu, Y. J. Liu, Q. Yu, Angiopoietin-3 is tethered on the cell surface via heparan sulfate proteoglycans. *J Biol Chem.* **2004**, *279*: 41179-41188.

66. A. Pulsipher, M. E. Griffin, S. E. Stone, L. C. Hsieh-Wilson, Long-lived engineering of glycans to direct stem cell fate. *Angew Chem Int Ed Engl.* **2015**, *54*: 1466-1470.

67. M. A. Hunt, M. J. Currie, B. A. Robinson, G. U. Dachs, Optimizing transfection of primary human umbilical vein endothelial cells using commercially available chemical transfection reagents. *J Biomol Tech.* **2010**, *21*: 66-72.

68. E. Campeau *et al.*, A versatile viral system for expression and depletion of proteins in mammalian cells. *PLoS One.* **2009**, *4*: e6529.

69. R. H. Kutner, X. Y. Zhang, J. Reiser, Production, concentration and titration of pseudotyped HIV-1-based lentiviral vectors. *Nat Protoc.* **2009**, *4*: 495-505.

70. S. L. Mayo, B. D. Olafson, W. A. Goddard III, DREIDING: a generic force field for molecular simulations. *J Phys Chem.* **1990**, *94*: 8897-8909.

71. V. W. Tak Kam, W. A. Goddard III, Flat-bottom strategy for improved accuracy in protein side-chain placements. *J Chem Theory Comput*. **2008**, *4*: 2160-2169.